AD-752 449

ELASTO-PLASTIC RESPONSE OF PLATES TO BLAST LOADING

Alan T. Barnard, et al

Loughborough University

Prepared for:

Army Research and Development Group (Europe)

September 1972

DISTRIBUTED BY:

NTIS
National Technical Information Service
U. S. DEPARTMENT OF COMMERCE
5285 Port Royal Road, Springfield Va. 22151

AD

ELASTO-PLASTIC RESPONSE OF PLATES TO BLAST LOADING.

Final Technical Report
(1st Year)

by

A. J. Barnard
P. W. Sharman

September, 1972.

EUROPEAN RESEARCH OFFICE
United States Army
London W.1., England.

Contract Number DAJA 37-71-C-4061

Department of Transport Technology,
University of Technology,
LOUGHBOROUGH,
Leicestershire,
ENGLAND.

DEPARTMENT OF TRANSPORT TECHNOLOGY

Loughborough University of Technology

DOCUMENT CONTROL DATA - R&D

(Security classification of title, body of abstract and indexing annotation must be entered when the overall report is classified)

1. ORIGINATING ACTIVITY (Corporate author) Department of Transport Technology, Univ. of Technology, LOUGHBOROUGH, Leics. Eng.	2a. REPORT SECURITY CLASSIFICATION UNCLASSIFIED 2b. GROUP N/A

3. REPORT TITLE

ELASTO-PLASTIC RESPONSE OF PLATES TO BLAST LOADING.

4. DESCRIPTIVE NOTES (Type of report and inclusive dates)

Final Technical Report, July 71 - August 72.

5. AUTHOR(S) (Last name, first name, initial)

Barnard, Alan, T.,
Sharman, Peter W.,

6. REPORT DATE	7a. TOTAL NO. OF PAGES	7b. NO. OF REFS
September 1972	58	71

8a. CONTRACT OR GRANT NO. DA JA37-71-C-4061 b. PROJECT NO. c d	9a. ORIGINATOR'S REPORT NUMBER(S) 72R06 9b. OTHER REPORT NO(S) (Any other numbers that may be assigned this report)

10. AVAILABILITY/LIMITATION NOTICES

[redacted]

Approved for public release, distribution unlimited.

11. SUPPLEMENTARY NOTES	12. SPONSORING MILITARY ACTIVITY
	U.S. Army R. & D. 6p (EUR) Box 15, FPO New York 09510

13. ABSTRACT

The report describes, in some detail, a proposed computer programme for the dynamic analysis of elasto-plastic, thin, isotropic plates of rectangular planform. Specific dynamic loading is considered which is appropriate to a blastwave, namely, a spatially constant pressure with infinitesimal rise time, decaying rapidly to a suction peak and finally to ambient conditions. Account is taken of the large deformations of the plate, and fixed or simply-supported boundary conditions. (U)

Much of the programme has been coded and step-by-step testing of the various subroutines is currently progressing. A flow chart of the main programme is given in Appendix I, and a statement of the subroutine testing completed as at the publication date is given in Appendix II.

(U)

14. KEY WORDS	LINK A		LINK B		LINK C	
	ROLE	WT	ROLE	WT	ROLE	WT
Structure						
Elasto-plastic Response						
Non-Linear Analysis						
Blast Loading						
Plates						

INSTRUCTIONS

1. ORIGINATING ACTIVITY: Enter the name and address of the contractor, subcontractor, grantee, Department of Defense activity or other organization (*corporate author*) issuing the report.

2a. REPORT SECURITY CLASSIFICATION: Enter the overall security classification of the report. Indicate whether "Restricted Data" is included. Marking is to be in accordance with appropriate security regulations.

2b. GROUP: Automatic downgrading is specified in DoD Directive 5200.10 and Armed Forces Industrial Manual. Enter the group number. Also, when applicable, show that optional markings have been used for Group 3 and Group 4 as authorized.

3. REPORT TITLE: Enter the complete report title in all capital letters. Titles in all cases should be unclassified. If a meaningful title cannot be selected without classification, show title classification in all capitals in parenthesis immediately following the title.

4. DESCRIPTIVE NOTES: If appropriate, enter the type of report, e.g., interim, progress, summary, annual, or final. Give the inclusive dates when a specific reporting period is covered.

5. AUTHOR(S): Enter the name(s) of author(s) as shown on or in the report. Enter last name, first name, middle initial. If military, show rank and branch of service. The name of the principal author is an absolute minimum requirement.

6. REPORT DATE: Enter the date of the report as day, month, year, or month, year. If more than one date appears on the report, use date of publication.

7a. TOTAL NUMBER OF PAGES: The total page count should follow normal pagination procedures, i.e., enter the number of pages containing information.

7b. NUMBER OF REFERENCES: Enter the total number of references cited in the report.

8a. CONTRACT OR GRANT NUMBER: If appropriate, enter the applicable number of the contract or grant under which the report was written.

8b, 8c, & 8d. PROJECT NUMBER: Enter the appropriate military department identification, such as project number, subproject number, system numbers, task number, etc.

9a. ORIGINATOR'S REPORT NUMBER(S): Enter the official report number by which the document will be identified and controlled by the originating activity. This number must be unique to this report.

9b. OTHER REPORT NUMBER(S): If the report has been assigned any other report numbers (*either by the originator or by the sponsor*), also enter this number(s).

10. AVAILABILITY/LIMITATION NOTICES: Enter any limitations on further dissemination of the report, other than those imposed by security classification, using standard statements such as:

(1) "Qualified requesters may obtain copies of this report from DDC."

(2) "Foreign announcement and dissemination of this report by DDC is not authorized."

(3) "U. S. Government agencies may obtain copies of this report directly from DDC. Other qualified DDC users shall request through ________________."

(4) "U. S. military agencies may obtain copies of this report directly from DDC. Other qualified users shall request through ________________."

(5) "All distribution of this report is controlled. Qualified DDC users shall request through ________________."

If the report has been furnished to the Office of Technical Services, Department of Commerce, for sale to the public, indicate this fact and enter the price, if known.

11. SUPPLEMENTARY NOTES: Use for additional explanatory notes.

12. SPONSORING MILITARY ACTIVITY: Enter the name of the departmental project office or laboratory sponsoring (*paying for*) the research and development. Include address.

13. ABSTRACT: Enter an abstract giving a brief and factual summary of the document indicative of the report, even though it may also appear elsewhere in the body of the technical report. If additional space is required, a continuation sheet shall be attached.

It is highly desirable that the abstract of classified reports be unclassified. Each paragraph of the abstract shall end with an indication of the military security classification of the information in the paragraph, represented as *(TS)*, *(S)*, *(C)*, or *(U)*.

There is no limitation on the length of the abstract. However, the suggested length is from 150 to 225 words.

14. KEY WORDS: Key words are technically meaningful terms or short phrases that characterize a report and may be used as index entries for cataloging the report. Key words must be selected so that no security classification is required. Identifiers, such as equipment model designation, trade name, military project code name, geographic location, may be used as key words but will be followed by an indication of technical context. The assignment of links, rules, and weights is optional.

TABLE OF CONTENTS

NOTATION

$[C]$	matrix relating stress coefficients and local nodal displacements
$[D]$	elasticity matrix
$[F_M]$	flow matrix defined by $\left(\frac{\partial F}{\partial \underset{\sim}{\sigma}}\right) = [F_M]\underset{\sim}{\sigma}$
H'	instantaneous slope of unaxial stress versus plastic strain plot at beginning of time increment
h	time increment
$[K]$	hybrid stiffness matrix
$[L]^j$	axes transformation matrix relating to a node
$[M]$	consistent mass matrix
$[N]$	compliance matrix
NELEM	total number of elements in idealization
NGPTS	number of Gaussian quadrature points per element
NNØDES	total number of nodes in idealization
NNPE	number of nodes per element
$\underset{\sim}{P}$	vector of applied nodal loads
$[Q]$	matrix relating elastic stress components and coefficients
$\underset{\sim}{q}, \dot{\underset{\sim}{q}}, \ddot{\underset{\sim}{q}}$	vector of nodal displacements, velocities and accelerations, respectively
$\Delta\underset{\sim}{q}_A, \Delta\dot{\underset{\sim}{q}}_A$	vectors used in accumulating incremental nodal displacements and velocities, respectively
$\underset{\sim}{R}$	vector of nodal pseudo-forces accounting for plasticity
$\underset{\sim}{S}$	vector of accumulative nodal pseudo-forces incorporating effects due to straining and large rotation from initial configuration
$[T]^e$	axes transformation matrix relating to an element
t	time co-ordinate
$[W]$	matrix of Gauss weights and co-ords over area of element
$[V]$	" " " " " " through thickness
x, y, z	rectangular space co-ordinates
$\underset{\sim}{\beta}$	vector of stress coefficients
κ	work hardening parameter
λ	proportionality constant in flow rule
$\underset{\sim}{\sigma}$	vector of stress components
σ_{u1}	uniaxial stress at first yield
$\bar{\sigma}^g$	equivalent stress at a station
$Y(\kappa)$	uniaxial yield stress subject to work hardening
$\underset{\sim}{\epsilon}$	vector of strain components
$\bar{\epsilon}_p^g$	equivalent plastic strain at a station
$\epsilon_{p,u}$	uniaxial plastic strain

Subscripts

e	elastic
eff	effective (i.e. uniaxial)
ep	elasto-plastic
L	relating to local axes
o	original
p	plastic
R	revised
ϵ	relating to additional straining effects
θ	relating to large rotation effects

Superscripts

e	elemental
g	at a Gauss Point
j	nodal
n	time step counter
T	matrix transposition

1. INTRODUCTION

The capability of large modern computers makes it possible to solve physical problems that defy a rigourous mathematical approach. One such problem of interest in engineering is the behaviour of thin plates subjected to blast loading. Obviously, the analysts of military systems have a keen interest, as do the engineers concerned with explosive forming.

The Finite Element method of stress analysis is ideally suited for large-scale computer systems and many successful analyses of complex structures have been reported. Steady progress from static to dynamic situations is apparent, and, more recently, the non-linear behaviour of both material and structure has commanded considerable attention.

Since elasto-plastic analysis is heavily dependant on stress prediction, it is essential to use a type of finite element formulation which has a good reputation for quite accurate stress analysis, without incurring excessive computer time by dealing with a fine element division. Such a formualtion is the "Hybrid" technique, developed by Pian, which falls between the strictly displacement methods and the "stress-mode" methods. Thus, the present research is centred on a well tested "hybrid" element, which may be triangular or quadrilateral in planform.

However, very considerable adaption of the element has proved necessary due to revised integration schemes through the volume in order to account for the partial plasticity within each element. The large deformations are taken into account by psuedo-forces acting at the nodes, and the non-linear equations of motion integrated by a Runge-Kutta predictor - corrector scheme.

2 A Survey of Solution Methods for Elasto-Plasticity Problems

This survey looks at recent work performed on the solution of structural problems involving non-linear material behaviour, and is restricted to elasto-plasticity. Other material non-linearities, such as creep, are not included and the reader is referred to the text by Zienkiewicz (1)* for discussion of these phenomena.

Firstly we shall briefly consider some of the latest experimental work performed in this area. A number of investigators have turned their attention to beams under blast loading. For example, Humphreys (2) has tested straight clamped beams, and Florence and Firth (3) have subjected both pinned and clamped rigid-plastic beams to uniformly distributed impulses. Grid frameworks have been investigated (4) as have perforated plates in plane-stress (5). Recently Jones et al. (6,7) performed tests on the dynamic behaviour of fully clamped rectangular plates and compared their results (6) with the theories of Martin (8) and Haythornthwaite and Shield (9).

Although progress was being made in the mathematical theory of plasticity (10,11) it was not until the advent of the high-speed digital computer, and in particular the application of the Finite-Element method to elasto-plastic materials, that the analysis of complex problems of this type became anything but very approximate. We shall, however, postpone discussion of this approach until we have considered some non-Finite-Element solutions. Usually major simplifying assumptions were made - often elastic effects were neglected (12,13) and perfect plasticity assumed (14.15). Prager (16) reviews the state of the art in the mid 1950's. At about this time Hopkins and Wang (17) had analysed circular perfectly plastic plates and compared results obtained using Tresca, von Mises and Parabolic (von Mises) yield conditions. Good agreement, especially for the simply-supported condition, between Tresca and von Mises was obtained. Ang and Lopez (18)

---

* such numbers are references

employed a grid analogy method and the usual sandwich plate assumptions in deriving their plate analysis. Deformable nodes represented average flexural and axial resistance, torsional elements modelled the in-plane sheer stresses and rigid bars transmitted the transverse shear forces induced by the flexural stresses. Results were given for the progression of the elasto-plastic boundary in square plates under various edge conditions.

Dynamic analyses of elasto-plastic plates have also been performed (12, 13). In 1959 Cox and Morland (19) considered a simply-supported square plate subjected to a pressure pulse, and later Florence (20) analysed clamped, circular plates under a rectangular blast pulse by assuming a rigid-plastic material yielding at the Tresca hexagon. Recently problems of combined material and geometric non-linearities have been tackled. Gerdeen et al.(21) have analysed shells of revolution under these conditions and Symonds and Jones (22) have investigated the behaviour of fully clamped beams composed of materials (particularly steels) which were strain-rate sensitive.

The Finite Difference approach has been used for some time to analyse elasto-plastic problems (e.g. 23, 24) sometimes in combination with large deflections. Balmer and Witmer (25) performed such an analysis on impulsively loaded beams, and, with high-energy metal forming in mind, the extension to thin shells has been made (26, 27). Leech et al.(26) presented results for a cylindrical panel and compared them with experiments, and Lindberg and Boyd (27) considered clamped, rigid-strain hardening shell membranes. It is however, evident that further work needs to be done in this particular field.

So far the Finite-Element method has been mentioned only fleetingly. Now we come to consider its application to the analysis of elasto-plastic structures. Although the Force approach (28, 29) has been used in this context, notably by Denke (30) and Lansing (31), the vast majority of workers have used the stiffness (displacement) method (32). It is

applications of this approach which will now be considered.

One of the most basic ways of solving the non-linear equations is by the Direct Iteration procedure. In this method the total load is applied to the structure and using the initial values of Young's Modulus, E, and Poisson's Ratio, ν, the elastic stresses and strains are computed. New values of E and ν are calculated according to the stress levels reached in each element, and then another full "elastic" analysis performed using these values. This procedure is repeated until the solution has converged. Figure 1a) shows a diagrammatic representation of this process as applied to a material with an elasto-plastic stress-strain curve which may be represented adequately by two straight lines. In 1963 the method was applied by Wilson (33) to 2-D structures and later used by Clough (34). These workers demonstrated that the Direct Iterative approach usually converges satisfactorily after 3 or 4 iterations. A completely different direct solution has been demonstrated by Mallet and Schmit (35). They use an Energy Search technique for a large deflection analysis and emphasise that the process is equally applicable to elasto-plasticity, although this point is disputed by Hofmeister et al.(50).

Probably the first method used for Finite-Element elasto-plastic analysis was the incremental Initial Strain approach introduced by Mendelson and Mason (36) in 1959. Padlog et al.(37) considered inelastic structures under cyclic, thermal and mechanical loading in 1960, and other pioneer work was performed by Gallagher et al.(38), Argyris (39) and Jensen et al.(40). The procedure is to apply the load incrementally and at each load step to treat the plastic strains produced as initital strains for the next increment. In this way pseudo-loads account for plasticity and it is

therefore necessary to modify only the right-hand-sides of equilibrium equations. This means that the elastic stiffness matrix is used throughout and thus needs to be built-up and inverted once only. Using the usual Finite-Element notation we may write the linear elastic stress-strain relationship for a material as

$$\underset{\sim}{\sigma} - \underset{\sim}{\sigma_o} = [D](\underset{\sim}{\epsilon} - \underset{\sim}{\epsilon_o}) \qquad \text{(i)}$$

In this approach it is the initial strain vector, $\underset{\sim}{\epsilon_o}$, which is adjusted to achieve a solution of the equilibrium equations

$$[K]\underset{\sim}{q} = \underset{\sim}{P} \qquad \text{(ii)}$$

where $\underset{\sim}{P}$ represents the vector 6f all forces due to external loads, initital strains, initial stresses etc. The procedure is shown diagrammatically in Figure 1b). If large increments of load are taken it can become necessary to iterate at each step in order to achieve high accuracy, but this can easily be avoided by taking the increments sufficiently small (39). A major disadvantage of the Initial Strain approach is that it breaks down for perfectly plastic materials because the strains in this case cannot be uniquely determined for prescribed stress levels.

A central problem in an Initial Strain analysis is the method used to compute the pseudo-forces. This is a much more crucial point in plate-bending than in 2-D analysis. Many non-Finite-Element plate-bending analyses assumed that at all points on the plate the entire thickness was either fully elastic or fully plastic (23, 18), and whilst this is the case for a plate of sandwich construction it is a very crude approximation for a solid plate. Using the Finite-Element method less drastic assumption can be made to overcome this problem. For example, Armen et al.(41) for their initial Strain analysis employed a triangular plate-bending element with quintic displacement functions and assumed the plastic strain to vary linearly from the upper and lower surfaces of the element to elastic-plastic boundaries within the cross-section. They further assumed a linear variation along the edges between adjacent nodes with a corresponding planar distribution throughout the area

of the element. Nodal strains were found by averaging values from surrounding elements. In this work the Romburg-Osgood stress-strain relationship (42) is employed, and so that the Bauschinger effect could be included for cyclic loading, the authors chose the Prager-Ziegler kinematic hardening theory of plasticity (16, 43, 44). However, recently this group of researchers have favoured numerical integration techniques both along the length and through the thickness of their shell of revolution (45). They have found 3 Gauss points generally adequate along the length. Through the thickness Simpson's integration employing up to 21 station was selected - the large number being required for the cyclic loading being considered in this work. The choice of Simpson's integration allowed the first, surface yielding to be detected, whereas Gaussian quadrature would have required yielding at interior points to take place before any contribution was registered. The strains at the integration points are now found by taking derivatives of the assumed displacement functions.

At present the most popular method for Finite-Element elasto-plastic analysis is the incremental Tangent Modulus or Variable Stiffness approach. This was initiated in 1965 by Pope (46) and Swedlow and Yang (47), and further developed for 2-D problems by Reyes and Deere (48) and Marcal and King (49) amongst others. In this method the load is again applied incrementally but now it is the matrix $[D]$ in equation (1) which is updated at each step to its tangential value, $[D_T]$, obtained from the effective stress-strain curve and corresponding to the stress state reached. This means that a new set of coefficients for the equilibrium equation (ii) must be found and a new inversion of this matrix performed at each load step. A diagram of the process is given as Figure 1c). A refinement occasionally employed to improve accuracy is described by Hofmeister et al. (50) in the context of a 2-D, large strain analysis. Here an equilibrium check is performed at each load step (or less frequently) and thus the nodal point equilibrium error reduced by using a Newton-Raphson interation procedure. A comparison between Initial Strain and

Tangent Modulus methods was given in 1968 by Marcal (51). He demonstrated that a larger load increment could be taken for a variable stiffness approach, but as the modifications to the equilibrium equations required at each step are considerably more extensive with this technique the overall efficiency for the two methods remains similar.

Constant stress and strain elements have often been used with the Tangent Modulus method for plane-stress elasto-plastic analyses. Richard and Blacklock (52) reported on such an element, whereas Felippa (53) described work using quadratic functions for both displacements. A linear variation of $[D_T]$ over the area was taken with values calculated at the vertices using average stresses from the elements at each node. The problem of evaluating the matrix $[D_T]$ for the Tangent Modulus approach is equivalent to the problem of computing the pseudo-forces for the Initial Strain approach. Recently Bergen and Clough (54) considered the Felippa approach for use with a quadrilateral plate-bending element, but concluded it to be over-complicated for this application. In addition, they expressed concern about assuming a continuous $[D_T]$ variation when this is frequently not so within the element. The approach selected by Bergen and Clough was to use 12 subtriangles per element and to take values of stresses at their centroids. Strip integration was used over the area and Gaussian quadrature through the thickness. As with the Initial Strain analysis by Levine et al. (45), the strains were obtained from the derivatives of the assumed displacement functions.

A good deal of work using the Tangent Modulus approach particularly applied to shells of revolution has been performed by Marcal (55, 56, 57, 58). He used the incremental theory of plasticity and the von Mises yield criterion. Isotropic strain hardening was assumed and a linear incremental elasto-plastic stress-strain relation obtained. Marcal (58) evaluated the stresses at the midway point of his axisymmetric shell element and used 11 numerical integration points through the thickness. In 1971 a dynamic analysis of beams and ring

was presented by Wu and Witmer (59). They assumed an elastic-perfectly plastic material and used a mechanical sublayer model. The equations of motion were solved by a time-wise, central-difference, numerical integration procedure using a time-step of 1 micro-second.

A further Finite-Element elasto-plastic method has recently been introduced by Zieniewicz et al.(60). This is known as the incremental Initial Stress approach, in which plasticity is accounted for by adjustments of the initial stress vector, $\underset{\sim}{\sigma_0}$, of equation (1). The approach is basically a modified Newton-Raphson procedure with the original value of the stiffness matrix being used throughout. Therefore most of the advantages of the Initial Strain approach are retained; indeed the two methods are in many ways parallel. However, the ability to analyse perfectly plastic materials is a notable additional advantage of the Initial Stress approach. For both these procedures, convergence may be accelerated by over-adjustment at each step. Such an accelerator for use with the Initial Stress approach has been developed by Nayak and Zienkiewicz (61). Another possibility is to occasionally update the stiffness matrix to its tangential value. Although the Initial Stress approach has been demonstrated to be convergent and efficient in plasticity problems (60), it may not be as suitable for problems involving large deformation (62).

Finally, we shall mention a very recent elasto-plastic analysis performed by Stricklin et al.(63) in which Finite Element and Finite Difference methods are combined. In this formulation the effect of the non-linearities are evaluated by means of Finite Difference expressions, but the general set-up of the analysis is Finite Element. The authors present results for shells of revolution and claim the computational procedure to be an order of magnitude faster than other analyses.

3. MATERIAL NON-LINEARITIES

3.1 General Theory of Plasticity

Firstly we will develop a general theory of plasticity to be used in the analysis. A yield surface can be defined by the general equation

$$F(\underset{\sim}{\sigma}, \kappa) = 0 \tag{1}$$

where κ is a work hardening parameter. Yielding can only occur when the stress components, $\underset{\sim}{\sigma}$, satisfy this criterion for the instantaneous value of κ. The particular yield surface which will be used is that proposed by von Mises. For a plate or shell where the normal-to-plane stress component, σ_z, is negligible, this is given by

$$F(\underset{\sim}{\sigma}, \kappa) = \left[\sigma_x^2 + \sigma_y^2 - \sigma_x\sigma_y + 3\left(\tau_{xy}^2 + \tau_{zx}^2 + \tau_{zy}^2\right)\right]^{\frac{1}{2}} - Y(\kappa) \tag{2}$$

where $Y(\kappa)$ is the corresponding value of the uniaxial yield stress.

The following incremental flow rule of plasticity is employed in the analysis:-

$$\underset{\sim}{d\epsilon}_p = \lambda\left(\frac{\partial F}{\partial \underset{\sim}{\sigma}}\right) \tag{3}$$

Here $\underset{\sim}{d\epsilon}_p$ represents the vector of incremental plastic strain components and λ is an unknown proportionality constant. Equation (3) is often referred to as the Normality Principle as it may be interpreted as the requirement that $\underset{\sim}{d\epsilon}_p$ must be normal to the yield surface in n-dimensional stress space.

Explicit formulations of the incremental plastic stress-strain relations have been derived by Yamada et al. (66) and Zienkiewicz et al. (60). They assume that for an infinitesimal stress increment the corresponding changes in strain may be divided into elastic and plastic parts, as

$$\underset{\sim}{d\epsilon} = \underset{\sim}{d\epsilon}_e + \underset{\sim}{d\epsilon}_p \tag{4}$$

or

$$\underset{\sim}{d\epsilon} = [D]^{-1}\underset{\sim}{d\sigma} + \lambda\left(\frac{\partial F}{\partial \underset{\sim}{\sigma}}\right) \tag{5}$$

By differentiation of the yield surface and the definition of

$$A = \frac{\partial F}{\partial K} \, dK \, \frac{1}{\lambda} \tag{6}$$

we can obtain the matrix equation

$$\begin{bmatrix} d\epsilon_x \\ d\epsilon_y \\ d\gamma_{xy} \\ d\gamma_{zx} \\ d\gamma_{zy} \\ 0 \end{bmatrix} = \left[\begin{array}{ccccc|c} & & & & & \frac{\partial F}{\partial \sigma_x} \\ & & & & & \frac{\partial F}{\partial \sigma_y} \\ & & [D]^{-1} & & & \frac{\partial F}{\partial \tau_{xy}} \\ & & & & & \frac{\partial F}{\partial \tau_{zx}} \\ & & & & & \frac{\partial F}{\partial \tau_{zy}} \\ \hline \frac{\partial F}{\partial \sigma_x} & \frac{\partial F}{\partial \sigma_y} & \frac{\partial F}{\partial \tau_{xy}} & \frac{\partial F}{\partial \tau_{zx}} & \frac{\partial F}{\partial \tau_{zy}} & A \end{array}\right] \begin{bmatrix} d\sigma_x \\ d\sigma_y \\ d\tau_{xy} \\ d\tau_{zx} \\ d\tau_{zy} \\ \lambda \end{bmatrix} \tag{7}$$

This type of relationship has been used with success by Marcal and King (49) in their Incremental Tangent Modulus approach. For our purposes however, it is more convenient to eliminate λ as demonstrated by Zienkiewicz et al. (60) to give

$$d\underset{\sim}{\sigma} = [D]_{ep} \, d\underset{\sim}{\epsilon} \tag{8}$$

where

$$[D]_{ep} = [D] - \frac{1}{S}[D]\left(\frac{\partial F}{\partial \underset{\sim}{\sigma}}\right)\left(\frac{\partial F}{\partial \underset{\sim}{\sigma}}\right)^T [D] \tag{9}$$

and

$$S = H' + \left(\frac{\partial F}{\partial \underset{\sim}{\sigma}}\right)^T [D] \left(\frac{\partial F}{\partial \underset{\sim}{\sigma}}\right) \tag{10}$$

Here H' is the slope of the uniaxial stress versus plastic strain plot at the value of the initial effective stress.

In the present case, using the von Mises yield surface given by equation (2) we have

$$\left(\frac{\partial F}{\partial \underset{\sim}{\sigma}}\right) = [F_M]\,\underset{\sim}{\sigma} \tag{11}$$

where

$$[F_M] = \frac{1}{Y(\kappa)}\begin{bmatrix} 1 & & & & \text{SYMM.} \\ -\frac{1}{2} & 1 & & & \\ 0 & 0 & 3 & & \\ 0 & 0 & 0 & 3 & \\ 0 & 0 & 0 & 0 & 3 \end{bmatrix} \tag{12}$$

If we define

$$\underset{\sim}{\eta} = [D]\,[F_M]\,\underset{\sim}{\sigma} \tag{13}$$

equation (10) becomes

$$S = H' + \underset{\sim}{\sigma}^T\,[F_M]^T\,\underset{\sim}{\eta} \tag{14}$$

and we can re-write equation (9) as

$$[D]_{ep} = [D] - \frac{1}{S}[D]\,\underset{\sim}{\eta}\,\underset{\sim}{\eta}^T \tag{15}$$

3.2 Finite Element Elasto-Plastic Procedure

The method chosen to account for plasticity effects is the incremental Initial Stress approach suggested by Zienkiewicz et al. (60) with adaptions to give compatibility with both the hybrid stiffness formulation and dynamic response analysis. The principal advantage of this formulation is that the original elastic material properties are used throughout the analysis with plasticity being included by means of a system of pseudo-forces acting at the nodes.

For each finite element, e, the subroutine ELPL is called

by the master programme to compute these forces, $\underset{\sim}{R}^{e}$, from the nodal displacements accumulated during a time increment. Gaussian quadrature (67) is used to obtain $\underset{\sim}{R}_{L}^{e}$ from residual (initial) stress values computed at discrete stations throughout the volume of the element.

In the original Initial Stress procedure proposed for static analysis, iteration was performed within each time increment until the pseudo-forces became negligibly small. This is, however, believed to be unnecessary for dynamic response analysis where these forces may be carried over to act during the next time increment.

3.3. The Elasto-Plastic Subroutine ELPL

A flowchart for this subroutine is included in Appendix I and the operations it performs will now be described. The process is represented diagramatically in Fig. 2.

Step 1

From the nodal displacements, $\Delta \underset{\sim}{q}_{n,L}^{e}$ accumulated for an element during a time step $n, n+1$ the change in the stress coefficients can be found as

$$\delta \underset{\sim}{\beta}^{e} = [C]^{e} \Delta \underset{\sim}{q}_{n,L}^{e} \tag{16}$$

Here the matrix $[C]^{e}$ has been derived during the normal hybrid stiffness computations.

Step 2

For a Gauss point, g, use the hybrid stress assumptions to obtain elastic increments of stress and strain,

$$\delta \underset{\sim}{\sigma}^{g} = [Q]^{g} \delta \underset{\sim}{\beta} \tag{17}$$

$$\delta \underset{\sim}{\epsilon}^{g} = [N] \delta \underset{\sim}{\sigma}^{g} \tag{18}$$

Add $\delta \underset{\sim}{\sigma}^{g}$ to the existing stress components, $\underset{\sim}{\sigma}^{g}$, to give $\underset{\sim}{\sigma}_{2}^{g}$.

Step 3

Test whether

$$F(\underset{\sim}{\sigma}_2^g, \kappa) \geqslant 0 \tag{19}$$

Here κ refers to its value at the start of the increment. If expression (19) is not satisfied then the increment is entirely elastic. Therefore up-date stress and strain components as

$$\underset{\sim}{\sigma}^{g,n+1} = \underset{\sim}{\sigma}_2^g \tag{20}$$

$$\underset{\sim}{\epsilon}^{g,n+1} = \underset{\sim}{\epsilon}^{g,n} + \delta\underset{\sim}{\epsilon}^g \tag{21}$$

and proceed to next Gauss station.

If expression (19) is satisfied, test whether

$$F(\underset{\sim}{\sigma}^g, \kappa) \geqslant 0 \tag{22}$$

using the stresses at the start of the increment. If expression (22) is also satisfied proceed to next step; if not interpolate for proportions of elastic stress and strain occuring above yield, revise $\delta\underset{\sim}{\sigma}^g$ and $\delta\underset{\sim}{\epsilon}^g$ to these values and update $\underset{\sim}{\sigma}^g$ and $\underset{\sim}{\epsilon}^g$ to the yield surface.

Step 4

Call the Subroutine HDASH to calculate H' and hence evaluate the scalor, S, from

$$S = H' + \underset{\sim}{\sigma}_2^{g,T}[F_M]^{g,T}\underset{\sim}{\eta}^g \tag{23}$$

and the elasto-plastic matrix

$$[D]_{ep} = [D] - \frac{1}{S}\underset{\sim}{\eta}^g\underset{\sim}{\eta}^{g,T} \tag{24}$$

Now the elasto-plastic stress increments may be calculated from

$$\delta\underset{\sim}{\sigma}_{ep}^g = [D]_{ep}\,\delta\underset{\sim}{\epsilon}^g \tag{25}$$

As equation (25) is valid for infinitesimal strain increments only, it is possible that for a finite step the stresses calculated will slightly exceed the yield surface. If this occurs the stresses, $\delta\underset{\sim}{\sigma}_{ep}^{g}$, are scaled down to the yield surface.

Step 5

Calculate the residual (initial) stress vector

$$\Delta\underset{\sim}{\sigma}^{g} = \delta\underset{\sim}{\sigma}^{g} - \delta\underset{\sim}{\sigma}_{ep}^{g} \tag{26}$$

and update the stress components as

$$\underset{\sim}{\sigma}^{g,n+1} = \underset{\sim}{\sigma}_{2}^{g} - \Delta\underset{\sim}{\sigma}^{g} \tag{27}$$

and the strain components as equation (21).

Step 6

Repeat Steps 2-5 for each Gauss station, hence evaluating, by Gaussian quadrature, the nodal pseudo-force vector in local co-ordinates as

$$\underset{\sim}{R}_{L}^{e,n+1} = \int_{V} \left([N]\,[Q]^{g}\,[C]^{e} \right)^{T} \Delta\underset{\sim}{\sigma}^{g}\, dV \tag{28}$$

The derivation of this expression is presented in Section 6.

Step 7

Transform pseudo-forces to global axes by performing

$$\underset{\sim}{R}^{j,n+1} = [L]^{j,n+1}\ \underset{\sim}{R}_{L}^{j,n+1} \tag{29}$$

and accumulating to form $\underset{\sim}{R}^{e,n+1}$

4. GEOMETRIC NONLINEARITIES

As soon as the maximum transverse displacement of the panel reaches about one-half the panel thickness the nonlinearity caused by the large displacements should be accounted

for. An incremental process originated by Argyris et al. (68, 69) is employed. The element stiffness matrices are systematically revised throughout the analysis by transforming the original matrices $[K]_0^e$ to the deformed orientations using the equation

$$[K]^e = [T]^{e,T} [K]_0^e [T]^e \tag{30}$$

This transformation accounts for gross movement of the whole element as a rigid body. In addition, the original equilibrium of each element is disturbed by the effects of straining and large rotations from the initial configuration, and to balance this a vector of cumulative nodal pseudo-forces, $\underset{\sim}{S}$, is included in the equations of motion of the system.

At the end of each step, the forces due to additional straining, $\delta S_\epsilon^{n,n+1}$, may be evaluated as

$$\delta \underset{\sim}{S}_\epsilon^{n,n+1} = [K]_R^{n+\frac{1}{2}} \Delta \underset{\sim}{q}_n \tag{31}$$

Here $[K]_R^{n+\frac{1}{2}}$ is the revised stiffness at the half-step and its significance in the solution procedure is explained in Section 5. In addition, forces incorporating large rotation effects and acting on each element are found by transforming the local pseudo-force vector, $\underset{\sim}{S}_L^{e,n}$, at the beginning of the time step as

$$\underset{\sim}{S}_\theta^{e,n+1} = \underset{\sim}{S}^{e,n} + \delta \underset{\sim}{S}_\theta^e = [T]^{e,n+1,T} \underset{\sim}{S}_L^{e,n} \tag{32}$$

Hence

$$\underset{\sim}{S}^{n+1} = \underset{\sim}{S}_\theta^{n+1} + \delta \underset{\sim}{S}_\epsilon^{n,n+1} \tag{33}$$

Thus it is now possible to include both material and geometric non-linearities into the analysis without entering the

necessarily time-consuming elemental stiffness routines more than once.

5. NUMERICAL INTEGRATION OF THE EQUATIONS OF MOTION

The equations of motion of the system can be written as

$$[M]\ddot{\underset{\sim}{q}} + [G]\dot{\underset{\sim}{q}} + [K]\underset{\sim}{q} = \underset{\sim}{P}(t) \tag{34}$$

To represent the non-linear system it is necessary to adopt a step-by-step procedure taking linear conditions to prevail throughout each small time interval. Thus during a particular time-step $n,n+1$ we can write.

$$[M]\delta\ddot{\underset{\sim}{q}}^{n,n+1} + [G]\delta\dot{\underset{\sim}{q}}^{n,n+1} + [K]\delta\underset{\sim}{q}^{n,n+1} = \delta\underset{\sim}{P}^{n,n+1} \tag{35}$$

The scheme selected for the numerical integration is an incremental predictor-corrector procedure using Runge-Kutta extrapolation techniques of $O(h^5)$ truncation errror. This formulation conveniently permits the inclusion of both the material and geometric non-linearities present.

For transient response analysis damping has very little effect on the general solution and for the present will be excluded from the analysis. If, however, in the future it is desired to include damping, only very slight modification of the programme would be required.

During one time-increment the following scheme of operations is performed:

Step 1

Compute the acceleration components vector at the beginning of the time step as

$$\ddot{\underset{\sim}{q}}^{n} = [M]^{-1}\left(\underset{\sim}{P}^{n} - \underset{\sim}{S}^{n} + \underset{\sim}{R}^{n}\right) \tag{36}$$

and hence evaluate storage vectors

$$\begin{aligned} \Delta\underset{\sim}{q}_{n} &= \dot{\underset{\sim}{q}}^{n} + \tfrac{1}{6}\underset{\sim}{V}_{1}^{n} \\ \Delta\dot{\underset{\sim}{q}}_{n} &= \underset{\sim}{V}_{1}^{n} = h\,\ddot{\underset{\sim}{q}}^{n} \end{aligned} \tag{37}$$

Step 2

Extrapolate for incremental displacements at the half-time interval as

$$\delta \underset{\sim}{q}^{n+\frac{1}{2}} = \frac{1}{2} h \dot{\underset{\sim}{q}}^{n} + \frac{1}{8} h \underset{\sim}{V}_1^{n} \tag{38}$$

and hence compute the corresponding accelerations as

$$\ddot{\underset{\sim}{q}}^{n+\frac{1}{2}} = [M]^{-1}\left(\underset{\sim}{P}^{n} - \underset{\sim}{S}^{n} + \underset{\sim}{R}^{n} - [K]^{n} \delta \underset{\sim}{q}^{n+\frac{1}{2}}\right) \tag{39}$$

Evaluate

$$\underset{\sim}{V}_2 = h \ddot{\underset{\sim}{q}}^{n+\frac{1}{2}} \tag{40}$$

and update storage vectors as

$$\Delta \underset{\sim}{q}_A = \Delta \underset{\sim}{q}_A + \frac{1}{6} \underset{\sim}{V}_2 \tag{41}$$

and

$$\Delta \dot{\underset{\sim}{q}}_A = \Delta \dot{\underset{\sim}{q}}_A + 2 \underset{\sim}{V}_2 \tag{42}$$

Step 3

Extrapolate for revised incremental displacements at the half-time interval as

$$\delta \underset{\sim}{q}_R^{n+\frac{1}{2}} = \frac{1}{2} h \dot{\underset{\sim}{q}}^{n} + \frac{1}{8} h \underset{\sim}{V}_2 \tag{43}$$

Hence compute

$$\underset{\sim}{q}_R^{n+\frac{1}{2}} = \underset{\sim}{q}^{n} + \delta \underset{\sim}{q}_R^{n+\frac{1}{2}} \tag{44}$$

and

$$\ddot{\underset{\sim}{q}}_R^{n+\frac{1}{2}} = [M]^{-1}\left(\underset{\sim}{P}^{n} - \underset{\sim}{S}^{n} + \underset{\sim}{R}^{n} - [K]^{n} \delta \underset{\sim}{q}_R^{n+\frac{1}{2}}\right) \tag{45}$$

Evaluate

$$\underset{\sim}{V}_3 = h \ddot{\underset{\sim}{q}}_R^{n+\frac{1}{2}} \tag{46}$$

and update storage vector $\Delta \underset{\sim}{q}_A$ to its final incremental value as

$$\Delta \underset{\sim}{q}_A = h\left(\Delta \underset{\sim}{q}_A + \frac{1}{6} \underset{\sim}{V}_3\right) \tag{47}$$

and update $\Delta \dot{\underset{\sim}{q}}_A$ as

$$\Delta \dot{\underset{\sim}{q}}_A = \Delta \dot{\underset{\sim}{q}}_A + 2 \underset{\sim}{V}_3 \tag{48}$$

Step 4

Extrapolate for incremental displacements at the end of the time-step as

$$\delta \underset{\sim}{q}^{n+1} = h \dot{\underset{\sim}{q}}^{n} + \frac{1}{2} h \underset{\sim}{V_3} \tag{49}$$

hence compute

$$\ddot{\underset{\sim}{q}}^{n+1} = [M]^{-1}\left(\underset{\sim}{P}^{n} - \underset{\sim}{S}^{n} + \underset{\sim}{R}^{n} - [K]_{R}^{n+\frac{1}{2}} \delta \underset{\sim}{q}^{n+1}\right) \tag{50}$$

Evaluate

$$\underset{\sim}{V_4} = h \ddot{\underset{\sim}{q}}^{n+1} \tag{51}$$

and update storage vector $\Delta \dot{\underset{\sim}{q}}_{A}$ to its final incremental value as

$$\Delta \dot{\underset{\sim}{q}}_{A} = \frac{1}{6}\left(\Delta \dot{\underset{\sim}{q}}_{A} + \underset{\sim}{V_4}\right) \tag{52}$$

Step 5

Update the displacement vector

$$\underset{\sim}{q}^{n+1} = \underset{\sim}{q}^{n} + \Delta \underset{\sim}{q}_{A} \tag{53}$$

retaining $\underset{\sim}{q}^{n}$ in store

Update velocity vector

$$\dot{\underset{\sim}{q}}^{n+1} = \dot{\underset{\sim}{q}}^{n} + \Delta \dot{\underset{\sim}{q}}_{A} \tag{54}$$

Step 6

Compute the nodal pseudo-forces incorporating geometric non-linearities, $\underset{\sim}{S}^{n+1}$, as described in Section 4.

Transform the incremental nodal displacements to local axes for each element using

$$\Delta \underset{\sim}{q}^{e}_{A,L} = [T]^{e,n} \Delta \underset{\sim}{q}^{e}_{A} \tag{55}$$

and hence update the vector of pseudo-forces for each element as

$$\underset{\sim}{S}_L^{e,n+1} = \underset{\sim}{S}_L^{e,n} + [K]_o^e \, \Delta \underset{\sim}{q}_{A,L}^e \qquad (56)$$

Step 7

For each element call the subroutine ELPL to calculate the nodal pseudo-forces accounting for plasticity, $R^{e,n+1}$, from $\Delta \underset{\sim}{q}_{A,L}^e$ as described in Section 3.3.

6. Derivation of Plasticity Pseudo-Force Expression

It has been demonstrated by Zienkiewicz (60) that, for an aelement, the vector of nodal pseudo-forces due to residual (initial) stresses can be expressed as

$$\underset{\sim}{R}_L^e = \int_V [B]^T \Delta \underset{\sim}{\sigma}^g \, dV \qquad (57)$$

where $[B]$ is the matrix relating strain and nodal displacements as

$$\underset{\sim}{\epsilon} = [B] \underset{\sim}{q}^e \qquad (58)$$

For the Hybrid approach we have

$$\underset{\sim}{\beta} = [C]^e \underset{\sim}{q}^e \qquad (59)$$

$$\therefore \underset{\sim}{\sigma} = [Q][C]^e \underset{\sim}{q}^e \qquad (60)$$

and

$$\underset{\sim}{\epsilon} = [N][Q][C]^e \underset{\sim}{q}^e \qquad (61)$$

Hence by comparison with equations (58) and (57) we can write

$$\underset{\sim}{R}_L^e = \int_V \left([N][Q][C]^e\right)^T \Delta \underset{\sim}{\sigma}^g \, dV \qquad (62)$$

7. Mass Matrix

It has been shown by Dungar et al. (65) that in order to achieve improved results in dynamic problems, the mass and hybrid stiffness matrices should be consistent with respect to assumed generalized displacement patterns. In the hybrid stiffness matrix these are taken along the element boundaries only, so it is necessary, when formulating the mass matrix, to extend the functions to cover the whole area of the element.

If q and u are respectively the vectors of generalized nodal and boundary displacements then they may be related by a matrix $[\bar{V}]$ as in the equation

$$\underset{\sim}{u} = [\bar{V}]\, \underset{\sim}{q} \tag{63}$$

If, also, the vector of generalized displacement within the element, $\underset{\sim}{d}$, is related to $\underset{\sim}{u}$ by:

$$\underset{\sim}{d} = [J]\, \underset{\sim}{u} \tag{64}$$

then the element mass matrix may be written as:

$$[M]^e = \rho [\bar{V}]^T \int_A [J]^T [J]\, dA\, [\bar{V}] \tag{65}$$

where

ρ = mass density of the material of the element.

If we put

$$[J_2] = \int_A [J]^T [J]\, dA \tag{66}$$

then

$$[M]^e = \rho [\bar{V}]^T [J_2] [\bar{V}] \quad . \tag{67}$$

The degrees of freedom at each node follow the ordering w, the transverse displacement and the two rotations θx and θy about the x and y axes respectively. For the general triangular element orientated with respect to the local axes as in Fig. 3, the $[\bar{V}]$ and $[J_2]$ matrices are as shown in Fig. 4 and 5 respectively. Transformation to global axes is achieved by the same process as the stiffness transformation.

8. BLAST-WAVE REPRESENTATION

The subroutine IMP calculates the loading vector, $\underset{\sim}{P}^{n}$, at time increment, n, from the impulsive forcing function, P(t). A number of different functions have been tested for their ability to represent the pressure-time curve for blast loading (fig. 6). Firstly, polynomial curve fitting was tried. This gave low root-mean-square errors for the higher order polynomials, but the representation of available experimental data gave alternatively over and under estimates along the length of the actual curve. Secondly, an exponential function given in Ref. 70 was tested:

$$P(t) = p_o \left(1 - t/t_f\right) e^{-t/t_f} \tag{68}$$

Here p_o is the initial (maximum) blast pressure and t is the intercept with the time axis. Fig. 3 shows that this function overestimates the absolute value of pressure throughout. Finally, a modification was made to the expression (68) to give

$$P(t) = p_o \frac{\left(1 - t/t_f\right)}{\left(1 + t/t_e\right)} e^{-t/t_f} \tag{69}$$

This function is seen to give much better agreement with the actual curve, and has been programmed as subroutine IMP. When values for p_o, t, t_f and t_e are input the subroutine will calculate the value of the loading vector $\underset{\sim}{P}^{n}$ at the time, t.

9. RECOMMENDATION FOR FURTHER WORK.

Whilst no directly applicable results have been obtained to date, the authors have been encouraged by the rapid development of the various subroutines, see Appendix II. The algorithmns employed for numerical integration are well known for their numerical stability, and the progressive nature of the spread of plasticity through each element should improve or other elasto-plastic methods.

It is recommended that the work is continued to fully exploit these developments.

References.

1. Zienkiewicz, O.C. 'The Finite Element Method in Engineering Science'. McGraw-Hill, 1971.

2. Humphreys, J.S. Plastic Deformation of Impulsively Loaded Clamped Beams. J. Appl. Mech., 32, p.7, 1965.

3. Florence, A.L., Firth, R.D. Rigid-Plastic Beams Under Uniformly Distributed Impulses. J. Appl. Mech., 32, p.481, 1965.

4. Reddy, D.V., Hendry, A.W. An Experimental Study of the Elasto-Plastic Behaviour of Certain Grid Frameworks. Exp. Mech., pp 120-125, 1965.

5. Theokaris, P.S., Marketos, E. Elasto-Plastic Analysis of Perforated Thin Strips of Strain-Hardening Material. J. Mech. Phys. Sci., 12, pp 377-390. 1964.

6. Jones, N., Uran, T.O., Tekin, S.A. The Dynamic Plastic Behaviour of Fully Clamped Rectangular Plates. Int. J. Solids Structures, 6, pp 1499-1512, 1970.

7. Jones, N., Griffin, R.N., Van Duzer, R.E. An Experimental Study into the Dynamic Plastic Behaviour of Wide Beams and Rectangular Plates. M.I.T. Report No. 69-12 1969.

8. Martin, J.B. Impulsive Loading Theorems for Rigid-Plastic Continua. Proc. A.S.C.E., 90, 27, 1964.

9.	Haythornthwaite, R.M. Shield, R.T.	A Note on the Deformable Region in Rigid-Plastic Structures. J. Mech. Phys. Solids, 6, p.127. 1958.
10.	Hill, R.	'The Mathematical Theory of Plasticity'. Oxford, London. 1964.
11.	Hoffman, O. Sachs, G.	'Introduction to the Theory of Plasticity'. McGraw-Hill. 1953.
12.	Wang, A.J. Hopkins, H.G.	On the Plastic Deformation of Built-in Circular Plates under Impulsive Loading. J. Mech. Phys. Solids, 3, pp 22 - 37 1954.
13.	Hopkins, H.G. Prager, W.	On the Dynamics of Plastic Circular Plates. J. Appl. Mech. Phys., ZAMP, 5, pp 317 - 330. 1954.
14.	Shull, H.E. Hu, L.W.	Load Carrying Capacities of Simply-Supported Rectangular Plates. J. Appl. Mech., 30 1963.
15.	Calladine, C.R.	'Engineering Plasticity' Pergamon Press.
16.	Prager, W.	The Theory of Plasticity: A Survey of Recent Achievements. James Clayton Lecture, Proc. I.M.E., 169. 1955.
17.	Hopkins, H.G.	Load-Carrying Capacities for Circular Plates of Perfectly-Plastic Material with Arbitrary Yield Condition. J. Mech. Phys. Solids, 3. 1954.

18. Ang, A.H.S.; Lopez, L.A. Discrete Model Analysis of Elastic-Plastic Plates. J. Eng. Mech. Div., Proc. A.S.C.E., EMI, pp 271-293. 1968.

19. Cox, A.D.; Morland, L.W. Dynamic Plastic Deformations of Simply-Supported Square Plates. J. Mech. Phys. Solids, 7. p.229. 1959.

20. Florence, A.L. Clamped, Circular, Rigid-Plastic Plates under Blast Loading. Trans. A.S.M.E. 1966.

21. Gerdeen, J.C.; Simonen, F.A.; Hunter, D.T. Large Deflection Analysis of Elasto-Plastic Shells using Numerical Integration. J. of A.I.A.A., 9, 6, 1971.

22. Symonds, P.S.; Jones, N. Impulsive Loading of Fully Clamped Beams with Finite Plastic Deflections. Brown Univ., Div. of Eng., N 00014-67-A-0191-0003/11, 1970.

23. Bhaumik, A.K.; Hanley, J.T. Elasto-Plastic Plate Analysis by Finite Difference. J. Struct. Div., Proc. A.S.C.E., ST5, pp 279-294. 1967.

24. Massonnet, C.; Cornelis. Theorie Generate des Plaques Elasto-Plastiques. Bulletin d'Information, Comite European du Breton, 56, Cement and Concrete Ass., London. 1966.

25.	Balmer, H.A. Witmer, E.A.	Theoretical-Experimental Correlation of Large Dynamic and Permanent Deformation of Impulsively loaded Simple Structures. FDL-TDR-64-108. AFFDL. Ohio, 1964.
26.	Leech, J.W. Witmer, E.A. Pian, T.H.H.	A Numerical Calculation Technique for Large Elasto-Plastic Transient Deformations of Thin Shells. J. of A.I.A.A., 6, p. 2352. 1968.
27.	Lindberg, C. Boyd, D.E.	Finite, Inelastic Deformations of Clamped Shell Membranes Subjected to Impulsive Loading. J. of A.I.A.A., 7, 2. 1969.
28.	Fraeijs de Veubeke, B.	'Matrix Methods of Structural Analysis'. Pergamon. 1964.
29.	Fraeijs de Veubeke, B.	Upper and Lower Bounds in Matrix Structural Analysis. AGARDograph, 72, pp 165-201. 1964.
30.	Denke, P.H.	Digital Analysis of Nonlinear Structures by the Force Method AGARDograph, 72 1964.
31.	Lansing, W. Jones, I.W. Ratner, P.	Nonlinear Analysis of Heated Cambered Wings by the Matrix Force Method. J. of A.I.A.A., 1, pp 1619-1626, 1963.
32.	Turner, M.J. Clough, R.W. Martin, H.C. Topp, L.J.	Stiffness and Deflection Analysis of Complex Structures. J. of Aero. Sci., 23, 9, pp 805-823, 854. 1956.

33. Wilson, E.L. — Finite-Element Analysis of 2-D Structures. Struct. Eng. Lab. Rep. No. 63-2, California Univ. Berkeley. 1963.

34. Clough, R.W. — The Finite-Element Method in Structural Mechanics. in 'Stress Analysis' ed. Zienkiewicz and Holister, Wiley. 1965.

35. Mallett, R.H., Schmit, L.A. Jr. — Nonlinear Structural Analysis by Energy Search. J. of Struct. Div., Proc. A.S.C.E. ST3, 1967.

36. Mendelson, A., Mason, S.S. — Practical Solution of Plastic Deformation Problems in the Elastic-Plastic Range. NASA TR R28 1959.

37. Padlog, J., Huff, R.D., Holloway, G.F. — The Unelastic Behaviour of Structures Subjected to Cyclic, Thermal and Mechanical Stressing Conditions. Bell Aero Systems Cr., Rep. WPADD TR 60-271. 1960.

38. Gallegher, R.H., Padlog, J., Bijlaard, P.P. — Stress Analysis of Heated Complex Shapes. ARS Journal, 32, pp 700-707. 1962.

39. Argyris. J.H. — Elasto-Plastic Matrix Displacement Analysis of 3-D Continua. J. of R.A.S. , TN 69, pp 633-635 1965.

40. Jenson, W.R., Falby, W.E., Prince, N. — Matrix Analyses for Anisotropic Inelastic Structures. AFFDL-TR-65-220 1965.

41. Armen, H. Jr.
Pifko, A.
Levine, H.S.
Finite Element Analysis of Structures in the Plastic Range.
NASA CR - 1649.
1971.

42. Romberg, W.
Osgood, W.R.
Description of Stress-Strain Curves by Three Parameters.
NACA TN 902.
1943.

43. Prager, W.
A New Method of Analysing Stresses and Strains in Work-Hardening Plastic Solids.
J. Appl. Mech., 23.
1956.

44. Ziegler, H.
A Modification of Prager's Hardening Rule.
Quart. Appl. Math., 17, 1.
1959.

45. Levine, H.
Armen, H. Jr.
Winter, R.
Theoretical and Experimental Investigation of the Large Reflection, Elasto-Plastic Behaviour of Orthotropic Shells of Revolution Under Cyclic Loading.
Nat. Symp. Comp. Struct. Anal. Des.,
G. Washington Univ.
1972.

46. Pope, G.G.
A Discrete Element Method for Analyses of Plane Elasto-Plastic Strain Problems.
R.A.E. Farnborough, TR 65028.
1965.

47. Swedlow, J.L.
Yang, W.H.
Stiffness Analysis of Elasto-Plastic Plates.
Calcit Report SM 65-10,
California I.T.,
1965.

48. Reyes, S.F.
Deere, D.U.
Elasto-Plastic Analysis of Underground Openings by the Finite Element Method.
Proc. 1st Int. Cong. Rock Mech., 11, pp 477-486.
Lisbon. 1966.

49. Marcal, P.V.; King, I.P. — Elasto-Plastic Analyses of 2-D Stress Systems by the Finite Element Method. Int. J. Mech., 9, 3, pp 143 - 155. 1967.

50. Hofmeister, L.D.; Greenbaum, G.A.; Evensen, D.A. — Large Strain, Elasto-Plastic, Finite Element Analysis. J. of A.I.A.A., 9, 7, 1971.

51. Marcal, P.V. — A Comparative Study of Numerical Methods in Elasto- Plastic Analysis. J. of A.I.A.A., 6, 1, pp 157-158. 1968.

52. Richard, R.M.; Blacklock, J.R. — Finite Element Analysis of Inelastic Structures. J. of A.I.A.A., 7, 3, 1969.

53. Felippa, C.A. — Refined Finite Element Analysis of Linear and Nonlinear 2-D Structures, Ph.D. Thesis, Univ. of California, Berkeley. 1966.

54. Bergen, P.G.; Clough, R.W. — Elasto-Plastic Analysis of Plates using the Finite Element Method. 3rd Conf. on Matrix Methods ib Structural Mechanic Wright-Patterson, A.F.B. Ohio. 1971.

55. Marcal, P.V. — Elasto-Plastic Analysis of Pressure Vessel Components. Proc. 1st P.V. and Piping Conf., ASME Comp. Seminar, Dallas, 1968.

56. Marcal, P. V. Finite Element Analyses of Combined Problems of Nonlinear Material and Geometric Behaviour. Comp. Appl, in Appl. Mechs., 1969.

57. Marcal, P. V. Large Deflection Analysis of Elasto-Plastic Plates and Shells. Proc. 1st Int. Conf. on P. V. Tech., Part I. 1969.

58. Marcal, P. V. Large Deflection Analysis of Elasto-Plastic Shells of Revolution. AIAA/ASME 10th Structures, Struct. Dyn., and Mat. Conf. 1969.

59. Wu, R. W. H.; Witmer, E. A. Finite Element Analysis of Large Elasto-Plastic Transient Deformations of simple Structure. J. of A.I.A.A. 9,9, 1971

60. Zienkiewicz, O. C.; Valliappan, S.; King, I. P. Elasto-Plastic Solution of Engineering Problems: Initial Stress, Finite Element Approach. Int. J. Num. Meth., 1, pp 75 -100, 1969.

61. Nayak, G. C.; Zienkiewicz, O. C. Elasto-Plastic Stress Analysis: A Generalisation using IsoParametric Elements and Various Constitutive Laws. Univ. of Wales, Civ. Eng., C/R148/71, 1971.

62. Zienkiewicz, O. C.; Nayak, G. C. A General Approach to the Problem of Large Deformation, and Plasticity using IsoParametric Elements. 3rd Conf. on Matrix Method in Struct. Mech., Wright-Patterson A.F.B., Ohio. 1971.

63. Stricklin, J. A.; Haisler, W. W.; Von Riesmann. Computation and Solution Procedures for Nonlinear Analysis by Combined Finite Element - Finite Difference Methods. Nat. Symp. Comp. Struct. Anal. and Des., G. Washington Univ., Washinton D.C., 1972

64. Dungar, R.; Severn, R. T.; Taylor, P. R. Vibration of Plate and Shell Structures using Triangular Finite Elements. J. of Strain Anal., 2, 1, pp 73-83, 1967.

65. Dungar, R. — The Dynamic Response of Elasto-Plastic and Geometrically Non-linear Structures to Impulsive Loading.
Symp. of Finite El. Tech. in Struct. Vibr., Southampton
1971.

66. Yamada, Y.
Yoshimura, N.
Sakurai, T. — Plastic Stress-Strain Matrix and Its Application to the Solution of Elasto-Plastic Problems by the Finite Element Method.
Int. J. Mech. Sci., 10, pp 343 - 354.
1968.

67. Kopal, Z. — Numerical Analysis.
Chapman and Hall Ltd.,
London.
1961.

68. Argyris, J. H.
Kelsey, S.
Kamel, H. — Matrix Method of Structural Analysis
AGARD-ograph 72
Pergamon Press,
1963.

69. Argyris, J. H. — Continua and Discontinua
Proc. Conf. Matrix Meth. Struct. Mech.,
Wright Patterson A.F.B., Ohio,
1965.

70. Niemi, R.
Rabenau, R. — Blast Effects on Space Vehicle Structures.
NASA TN D-2945,
1966.

71. Hammer, P. C.
Marlowe, O. P.
Stroud, A. H. — Numerical Integration over Simplexes and Cones.
Maths. Tables Aids Comp., 10, 130-137.
1956.

APPENDIX I - FLOWCHARTS

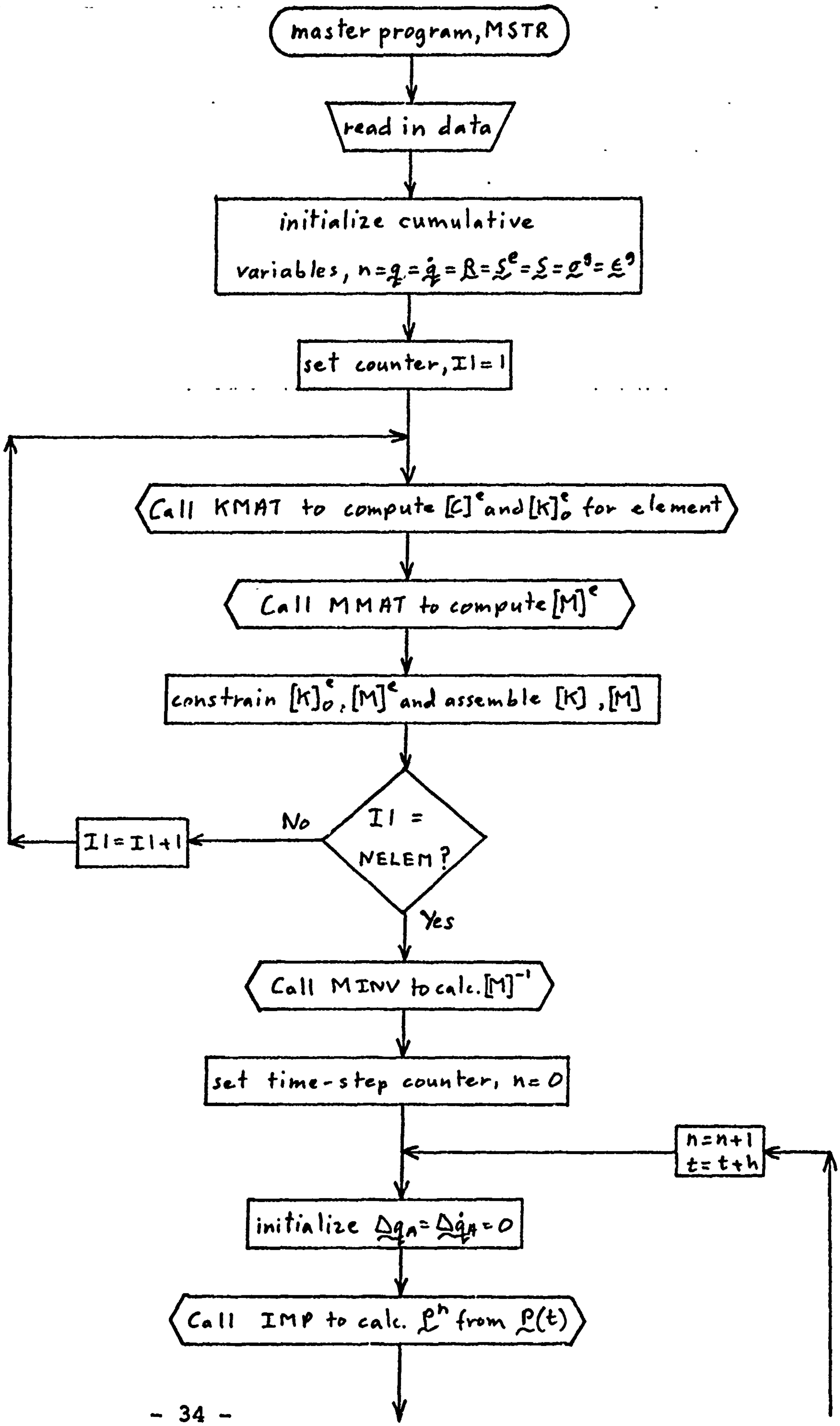

$$\boxed{\text{eval. } \ddot{q}^{n} = [M]^{-1}\left(P^{n} - S^{n} + R^{n}\right)}$$

$$\downarrow$$

$$\boxed{V_1 = h\,\ddot{q}^{n}}$$

$$\downarrow$$

$$\boxed{\text{extrap. } \delta q^{n+\frac{1}{2}} = \tfrac{1}{2} h\,\dot{q}^{n} + \tfrac{1}{8} h\,V_1^{n}}$$

$$\downarrow$$

$$\boxed{\Delta q_A = \dot{q}^{n} + \tfrac{1}{6} V_1}$$

$$\downarrow$$

$$\boxed{\Delta \dot{q}_A = V_1}$$

$$\downarrow$$

$$\boxed{\text{eval. } \ddot{q}^{n+\frac{1}{2}} = [M]^{-1}\left(P^{n} - S^{n} + R^{n} - [K]^{n}\,\delta q^{n+\frac{1}{2}}\right)}$$

$$\downarrow$$

$$\boxed{V_2 = h\,\ddot{q}^{n+\frac{1}{2}}}$$

$$\downarrow$$

$$\boxed{\Delta q_A = \Delta q_A + \tfrac{1}{6} V_2}$$

$$\downarrow$$

$$\boxed{\Delta \dot{q}_A = \Delta \dot{q}_A + 2 V_2}$$

$$\downarrow$$

$$\boxed{\text{extrap. } \delta q_R^{n+\frac{1}{2}} = \tfrac{1}{2} h\,\dot{q}^{n} + \tfrac{1}{8} h\,V_2^{n+\frac{1}{2}}}$$

$$\downarrow$$

$$\boxed{q_R^{n+\frac{1}{2}} = q^{n} + \delta q_R^{n+\frac{1}{2}}}$$

$$\downarrow$$

$$\boxed{\text{eval. } \ddot{q}_R^{n+\frac{1}{2}} = [M]^{-1}\left(P^{n} - S^{n} + R^{n} - [K]^{n}\,\delta q_R^{n+\frac{1}{2}}\right)}$$

$$\downarrow$$

$$\boxed{V_3 = h\,\ddot{q}_R^{n+\frac{1}{2}}}$$

$$\downarrow$$

$$\boxed{\Delta q_A = \left(\Delta q_A + \tfrac{1}{6} V_3\right) h}$$

$$\downarrow$$

$$\boxed{\Delta \dot{q}_A = \Delta \dot{q}_A + 2 V_3}$$

$$\downarrow$$

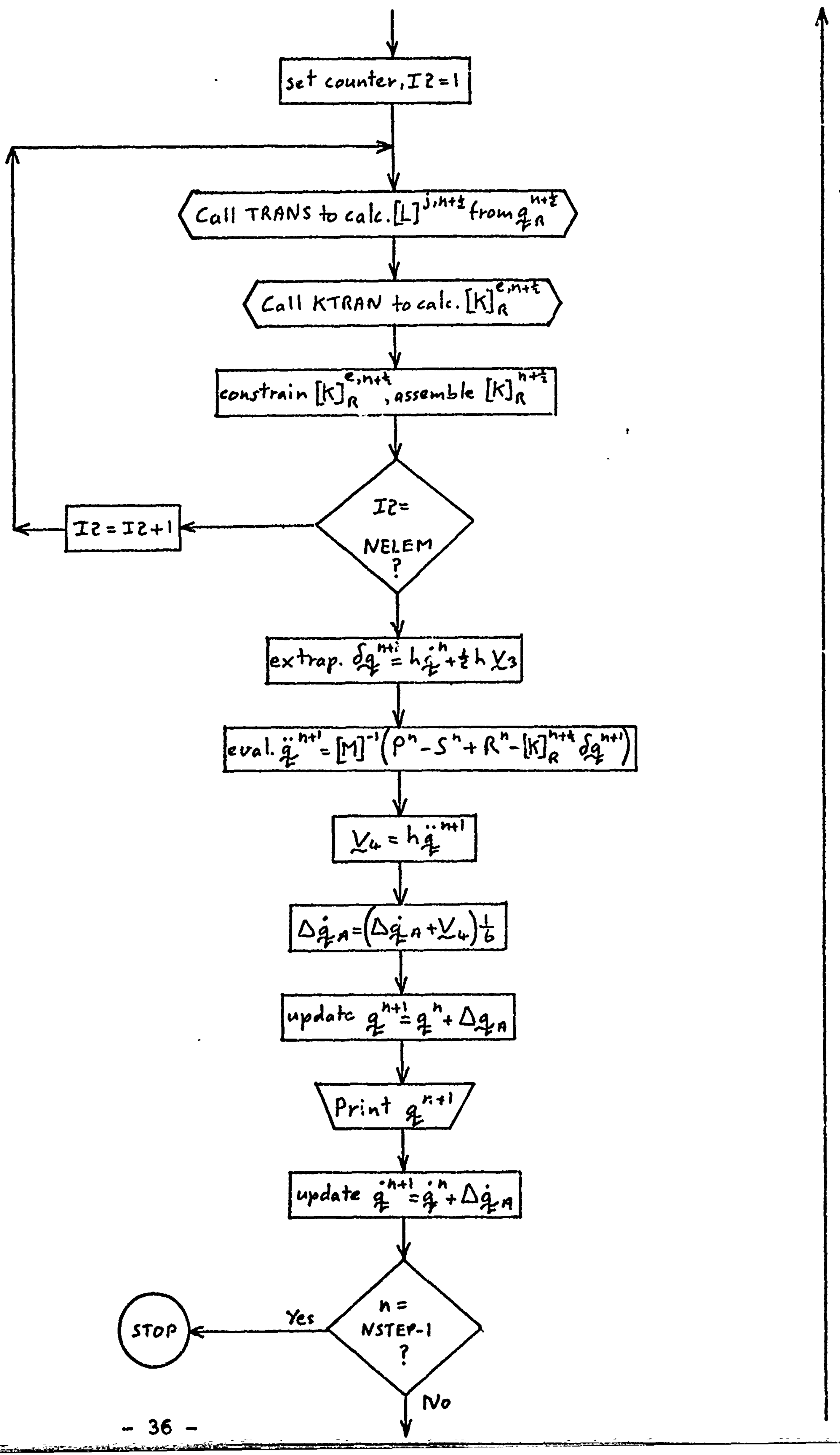
set counter, I2 = 1
Call TRANS to calc. $[L]^{j,n+\frac{1}{2}}$ from $q_R^{n+\frac{1}{2}}$
Call KTRAN to calc. $[K]_R^{e,n+\frac{1}{2}}$
constrain $[K]_R^{e,n+\frac{1}{2}}$, assemble $[K]_R^{n+\frac{1}{2}}$
I2 = NELEM ?
I2 = I2+1
extrap. $\delta q^{n+1} = h\dot{q}^n + \frac{1}{2} h V_3$
eval. $\ddot{q}^{n+1} = [M]^{-1}(P^n - S^n + R^n - [K]_R^{n+\frac{1}{2}} \delta q^{n+1})$
$V_4 = h\ddot{q}^{n+1}$
$\Delta\dot{q}_A = (\Delta\dot{q}_A + V_4)\frac{1}{6}$
update $q^{n+1} = q^n + \Delta q_A$
Print q^{n+1}
update $\dot{q}^{n+1} = \dot{q}^n + \Delta\dot{q}_A$
n = NSTEP-1 ?
Yes
STOP
No

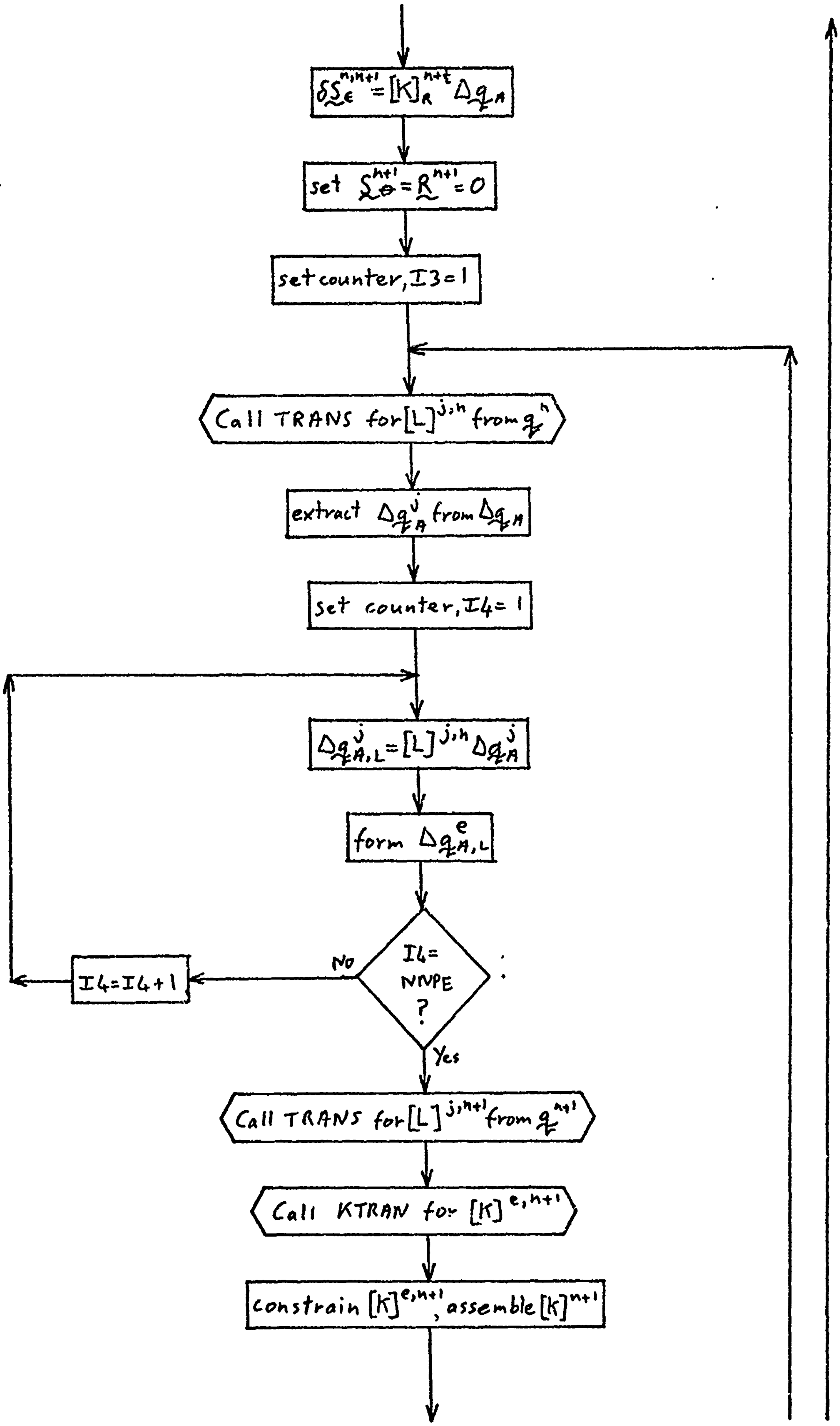
$\delta \underset{\sim}{S}_\epsilon^{n,n+1} = [K]_R^{n+1} \Delta q_A$
set $\underset{\sim}{S}_\theta^{n+1} = \underset{\sim}{R}^{n+1} = 0$
set counter, I3=1
Call TRANS for $[L]^{j,n}$ from q^n
extract Δq_A^j from Δq_A
set counter, I4=1
$\Delta q_{A,L}^j = [L]^{j,n} \Delta q_A^j$
form $\Delta q_{A,L}^e$
I4= NVPE ?
No
I4=I4+1
Yes
Call TRANS for $[L]^{j,n+1}$ from q^{n+1}
Call KTRAN for $[K]^{e,n+1}$
constrain $[K]^{e,n+1}$, assemble $[K]^{n+1}$

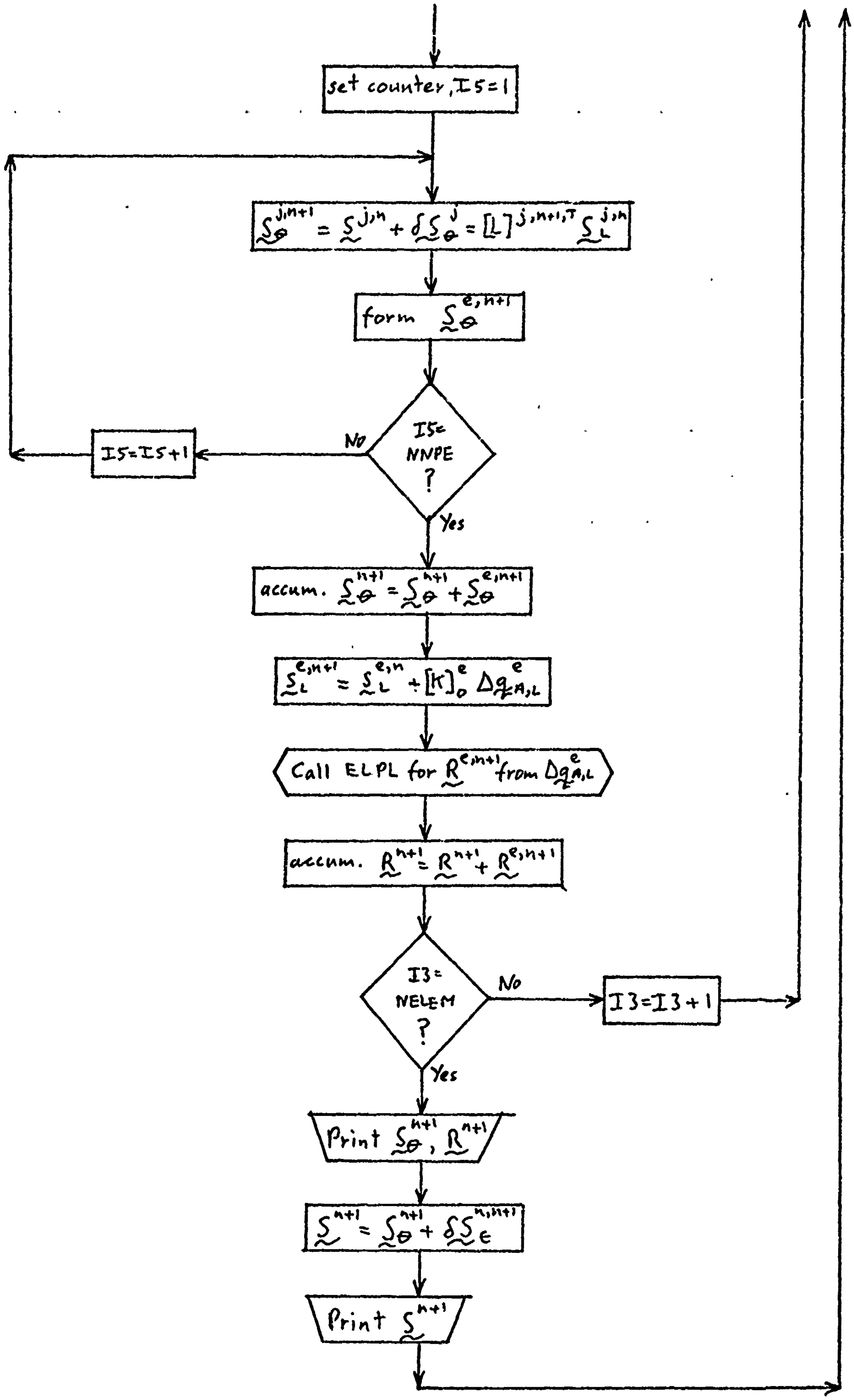

set counter, I5=1
$S_\theta^{j,n+1} = S^{j,n} + \delta S_\theta^{j} = [L]^{j,n+1,T} S_L^{j,n}$
form $S_\theta^{e,n+1}$
I5= NNPE ?
No
I5=I5+1
Yes
accum. $S_\theta^{n+1} = S_\theta^{n+1} + S_\theta^{e,n+1}$
$S_L^{e,n+1} = S_L^{e,n} + [K]_o^e \, \Delta q_{A,L}^e$
Call ELPL for $R^{e,n+1}$ from $\Delta q_{A,L}^e$
accum. $R^{n+1} = R^{n+1} + R^{e,n+1}$
I3= NELEM ?
No
I3=I3+1
Yes
Print S_θ^{n+1}, R^{n+1}
$S^{n+1} = S_\theta^{n+1} + \delta S_\epsilon^{n,n+1}$
Print S^{n+1}

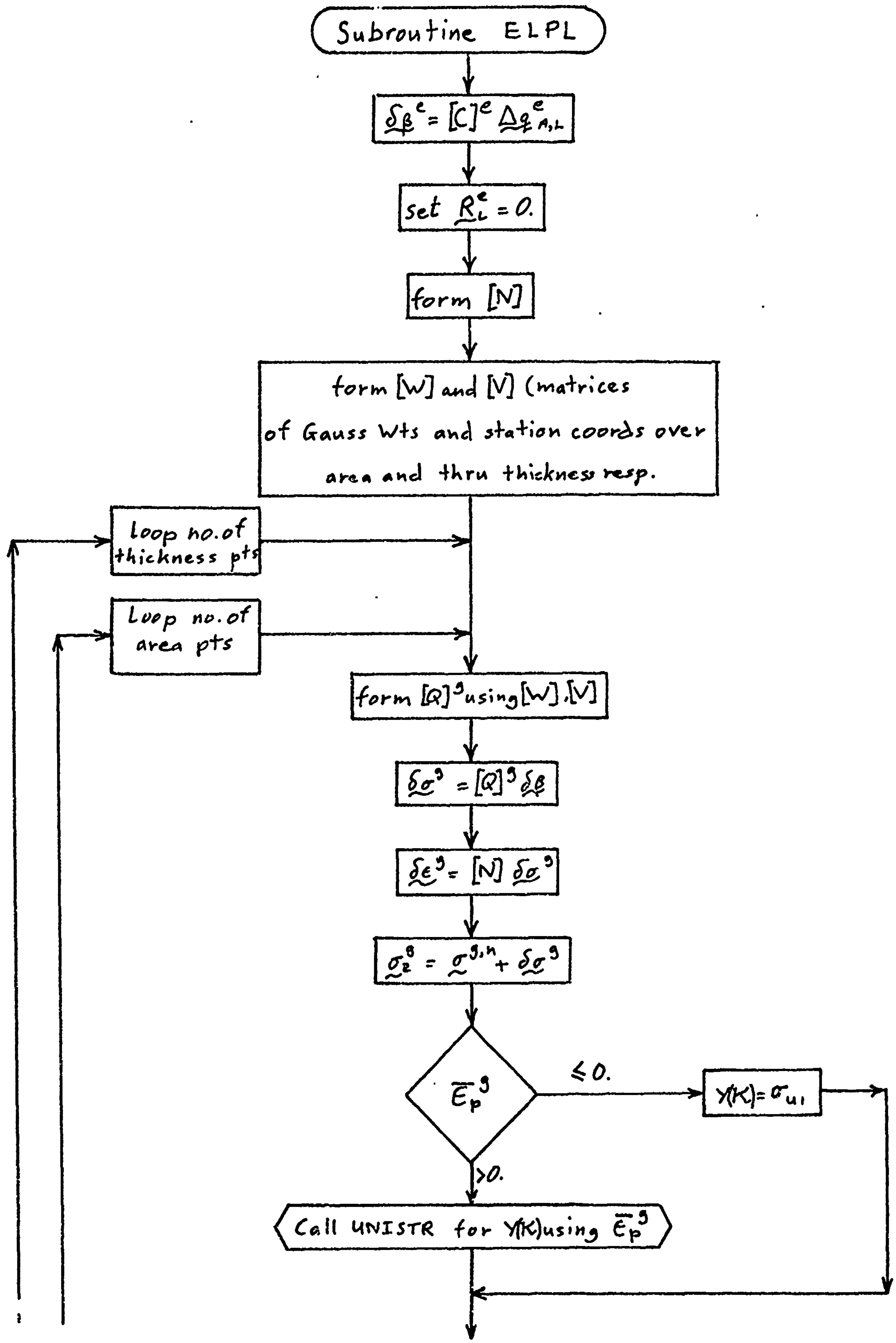
Subroutine ELPL
$\underset{\sim}{\delta\beta}^e = [C]^e \underset{\sim}{\Delta q}^e_{A,L}$
set $\underset{\sim}{R}^e_L = 0.$
form [N]
form [W] and [V] (matrices of Gauss Wts and station coords over area and thru thickness resp.
loop no. of thickness pts
Loop no. of area pts
form $[Q]^g$ using [W], [V]
$\underset{\sim}{\delta\sigma}^g = [Q]^g \underset{\sim}{\delta\beta}$
$\underset{\sim}{\delta\epsilon}^g = [N]\, \underset{\sim}{\delta\sigma}^g$
$\underset{\sim}{\sigma}^g_2 = \underset{\sim}{\sigma}^{g,n} + \underset{\sim}{\delta\sigma}^g$
$\bar{\epsilon}_p^g$
$\leq 0.$
$Y(K) = \sigma_{u1}$
$>0.$
Call UNISTR for Y(K) using $\bar{\epsilon}_p^g$

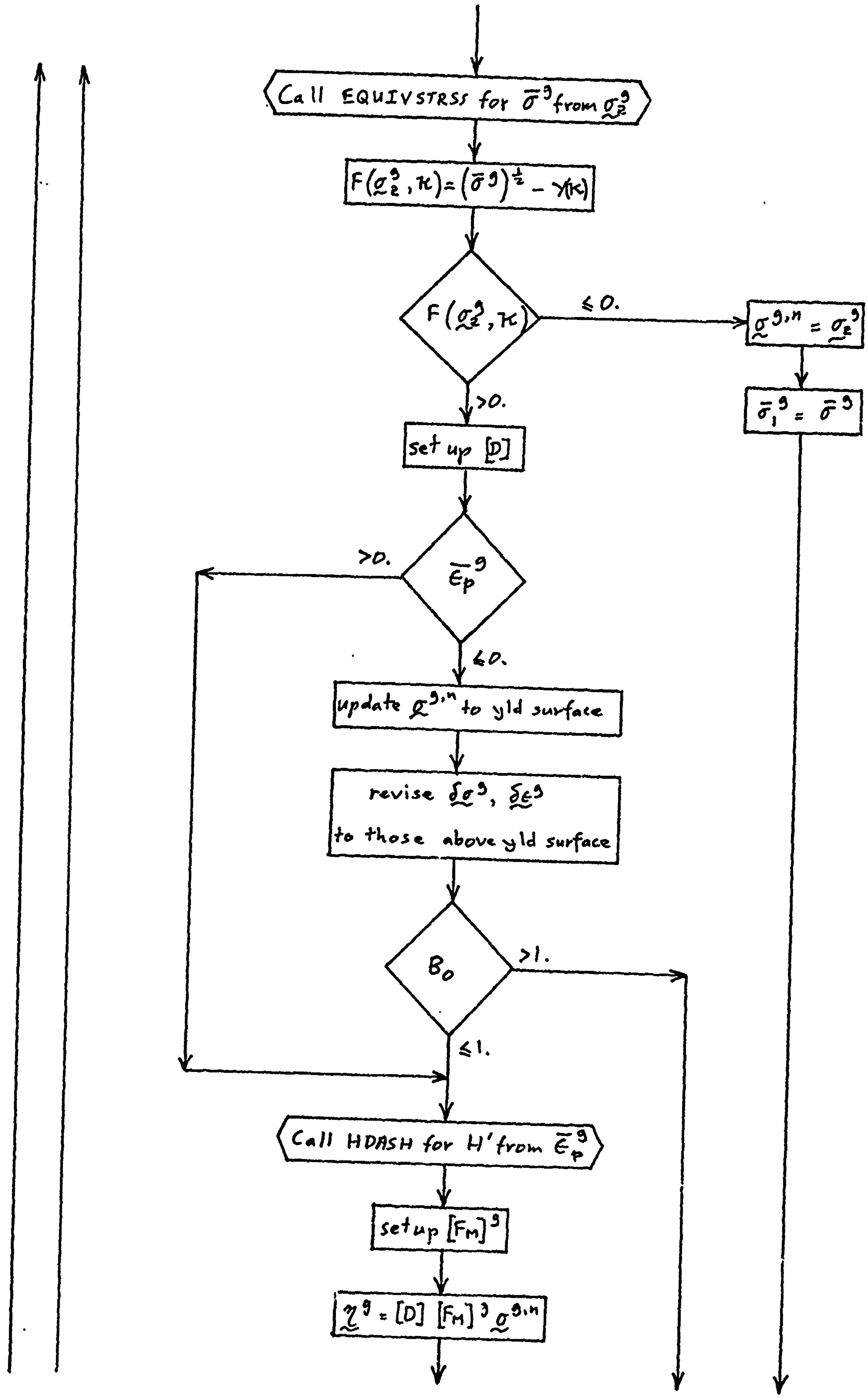

Call EQUIVSTRSS for $\bar{\sigma}^g$ from $\underset{\sim}{\sigma}_2^g$
$F(\underset{\sim}{\sigma}_2^g, \kappa) = (\bar{\sigma}^g)^{\frac{1}{2}} - Y(\kappa)$
$F(\underset{\sim}{\sigma}_2^g, \kappa)$
≤0.
$\underset{\sim}{\sigma}^{g,n} = \underset{\sim}{\sigma}_2^g$
$\bar{\sigma}_1^g = \bar{\sigma}^g$
>0.
set up [D]
>0.
$\bar{\epsilon}_p^g$
≤0.
update $\underset{\sim}{\sigma}^{g,n}$ to yld surface
revise $\underset{\sim}{\delta\sigma}^g$, $\underset{\sim}{\delta\epsilon}^g$
to those above yld surface
B_0
>1.
≤1.
Call HDASH for H' from $\bar{\epsilon}_p^g$
setup $[F_M]^g$
$\underset{\sim}{\eta}^g = [D]\ [F_M]^g\ \underset{\sim}{\sigma}^{g,n}$

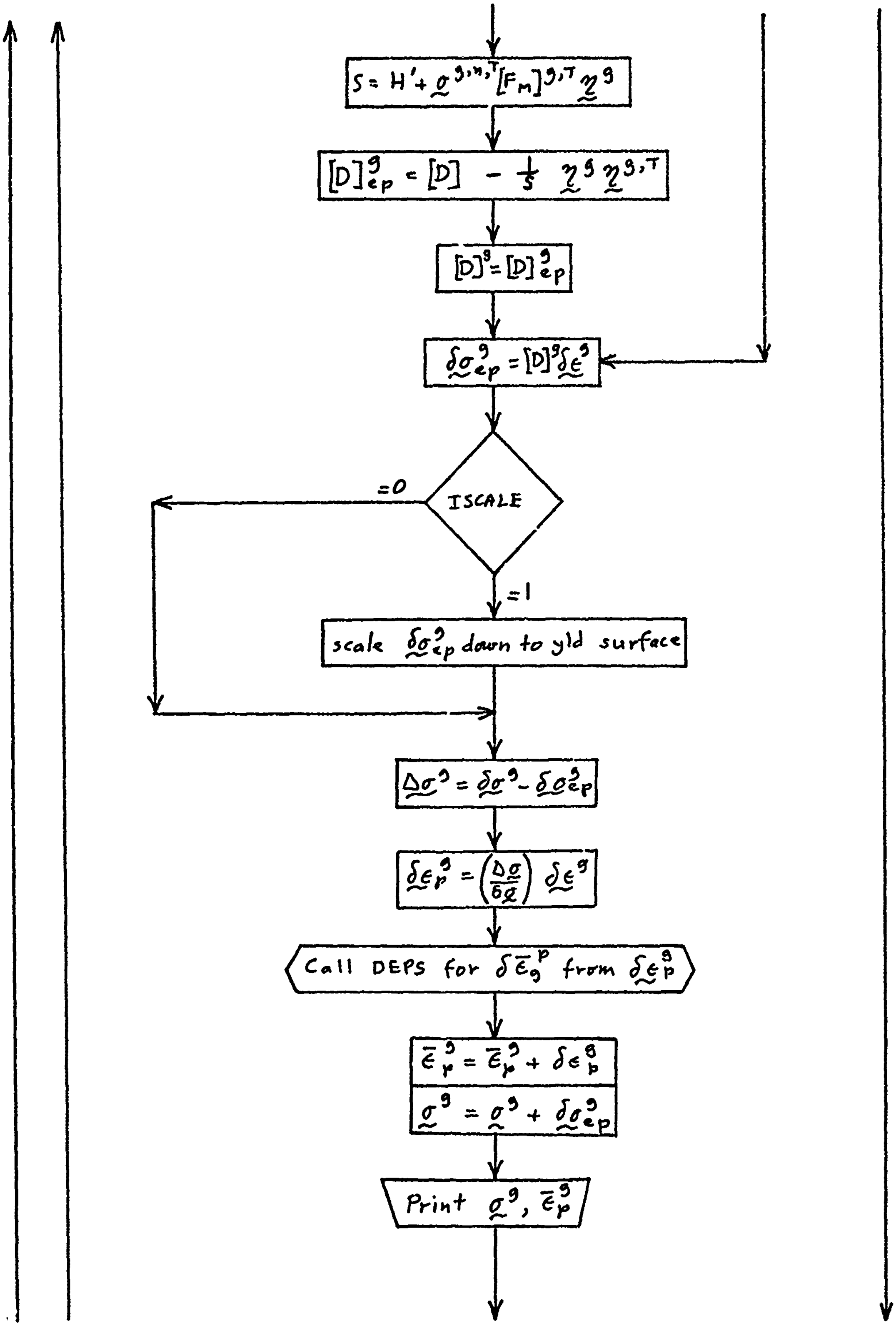

$S = H' + \sigma^{g,n,T}[F_m]^{g,T} \eta^g$
$[D]^g_{ep} = [D] - \frac{1}{S} \eta^g \eta^{g,T}$
$[D]^g = [D]^g_{ep}$
$\delta\sigma^g_{ep} = [D]^g \delta\epsilon^g$
ISCALE
=0
=1
scale $\delta\sigma^g_{ep}$ down to yld surface
$\Delta\sigma^g = \delta\sigma^g - \delta\sigma^g_{ep}$
$\delta\epsilon^g_p = \left(\frac{\Delta\sigma}{\delta\sigma}\right) \delta\epsilon^g$
Call DEPS for $\delta\bar{\epsilon}^p_g$ from $\delta\epsilon^g_p$
$\bar{\epsilon}^g_p = \bar{\epsilon}^g_p + \delta\epsilon^g_p$
$\sigma^g = \sigma^g + \delta\sigma^g_{ep}$
Print σ^g, $\bar{\epsilon}^g_p$

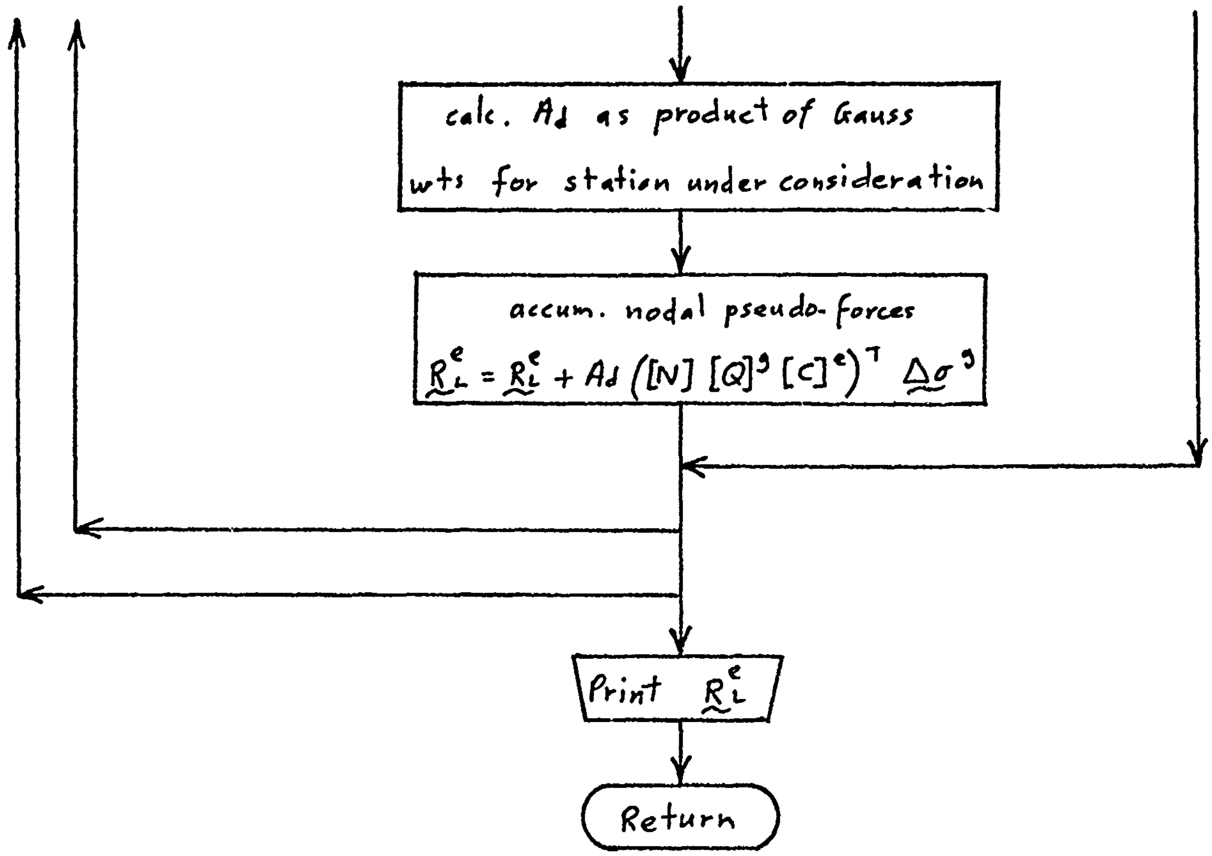
calc. Ad as product of Gauss wts for station under consideration
accum. nodal pseudo-forces
$\underset{\sim}{R}_L^e = \underset{\sim}{R}_L^e + Ad\left([N]\,[Q]^g\,[C]^e\right)^T \underset{\sim}{\Delta\sigma}^g$
Print $\underset{\sim}{R}_L^e$
Return

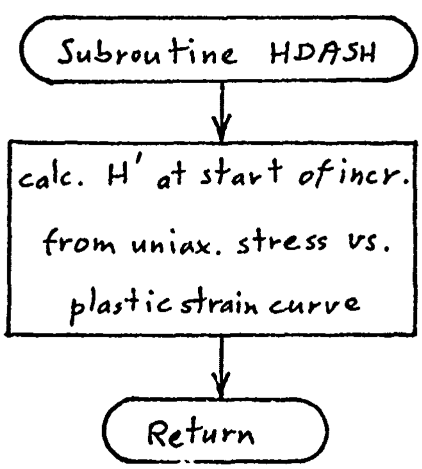
Subroutine HDASH
calc. H' at start of incr. from uniax. stress vs. plastic strain curve
Return

Subroutine UNISTR

↓

calc. Y(K) for a partic. $\bar{\epsilon}_p$ from uniax. stress vs. plastic strain curve

↓

Return

Subroutine EQUIVSTRSS

↓

calc. $\bar{\sigma}^g$ at a point from the stress vector $\underset{\sim}{\sigma}_n^g$

↓

Return

Subroutine DEPS

↓

calc. $\delta\bar{\epsilon}_p$ at a point from incr. strain vector $\underset{\sim}{\delta\epsilon}_p$

↓

Return

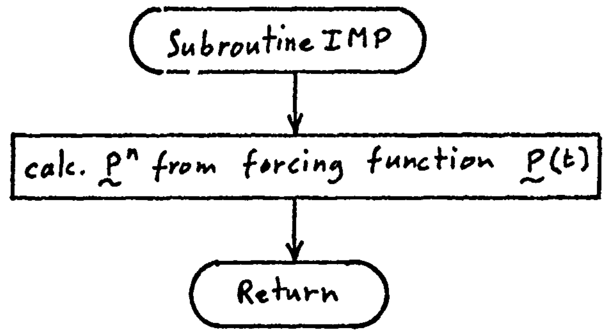
Subroutine IMP
calc. $\underset{\sim}{P}^n$ from forcing function $\underset{\sim}{P}(t)$
Return

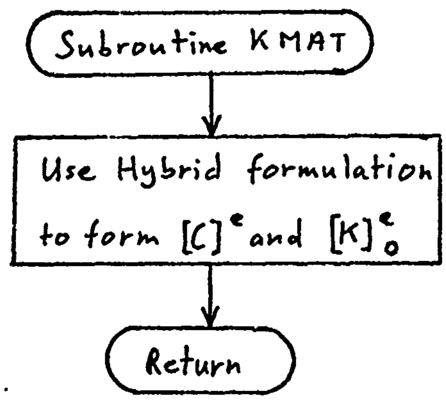
Subroutine KMAT
Use Hybrid formulation to form $[C]^e$ and $[K]^e_o$
Return

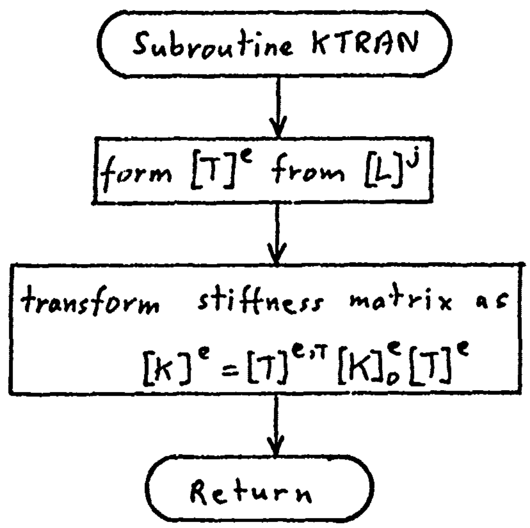
Subroutine KTRAN
form $[T]^e$ from $[L]^j$
transform stiffness matrix as $[K]^e = [T]^{e,T} [K]^e_o [T]^e$
Return

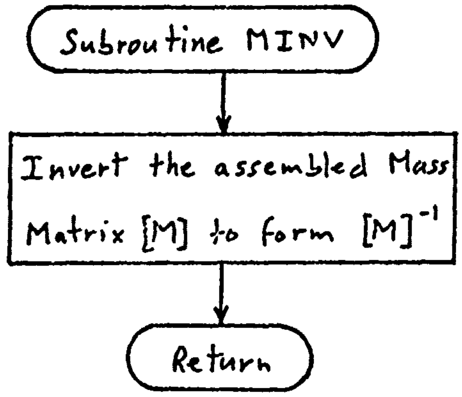
Subroutine MINV
Invert the assembled Mass Matrix [M] to form [M]$^{-1}$
Return

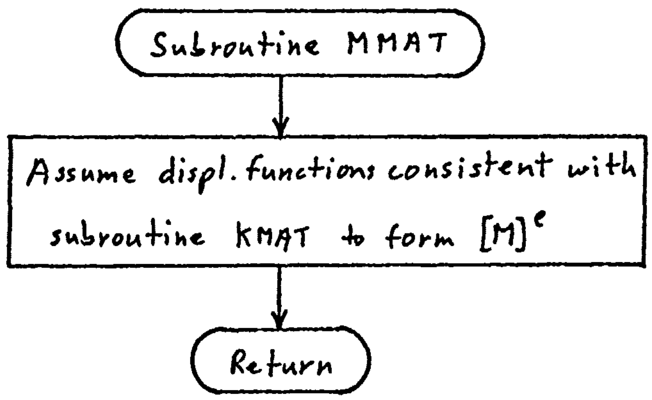
Subroutine MMAT
Assume displ. functions consistent with subroutine KMAT to form [M]^{e}
Return

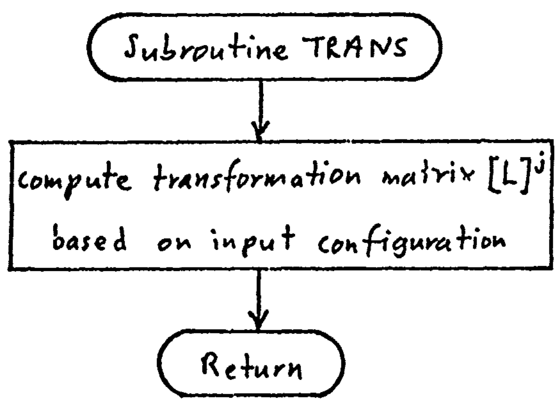
Subroutine TRANS
compute transformation matrix [L]^{j} based on input configuration
Return

APENDIX II - SUBROUTINES TESTED AS AT 31.8.'72

Subroutine EQUIVSTRESS

Given a vector of stress components, at a Gauss station this subroutine will calculate the value of the corresponding equivalent stress, $\bar{\sigma}^g$, as

$$\bar{\sigma}^g = \left\{ \left(\sigma_x^g\right)^2 + \left(\sigma_y^g\right)^2 - \sigma_x^g \sigma_y^g + 3\left[\left(\tau_{xy}^g\right)^2 + \left(\tau_{zx}^g\right)^2 + \left(\tau_{zy}^g\right)^2\right]\right\}^{\frac{1}{2}} \qquad \text{(A.1)}$$

Subroutine DEPS

This subroutine calculates the incremental value of the equivalent plastic strain, $\delta\bar{\epsilon}_p^g$, at a Gauss station, based on a vector of corresponding incremental plastic strain components, $\underset{\sim}{\delta\epsilon}_p^g$.

$$\delta\bar{\epsilon}_p^g = \left(\frac{2}{3}\left[\left(\delta\epsilon_{p,x}^g\right)^2 + \left(\delta\epsilon_{p,y}^g\right)^2 + \frac{1}{2}\left\{\left(\delta\gamma_{p,xy}^g\right)^2 + \left(\delta\gamma_{p,zx}^g\right)^2 + \left(\delta\gamma_{p,zy}^g\right)^2\right\}\right]\right)^{\frac{1}{2}} \qquad \text{(A.2)}$$

Subroutine UNISTR

The equation of the uniaxial stress ($Y(\kappa)$) versus uniaxial plastic strain ($\epsilon_{p,u}$) curve is taken to be

$$\epsilon_{p,u} = A\left(Y(\kappa) - \sigma_{u1}\right)^B \qquad \text{(A.3)}$$

where σ_{u1} is the uniaxial stress at first yield.

When given values for A, B, σ_{u1} and $\epsilon_{p,u}$ subroutine UNISTR will calculate the value of the uniaxial stress, $Y(\kappa)$. This, together with the equivalent stress, $\bar{\sigma}$, is required in the evaluation of the yield surface function at a point, as

$$F(\underset{\sim}{\sigma}, \kappa) = \bar{\sigma} - Y(\kappa) \qquad \text{(A.4)}$$

Subroutine HDASH

This subroutine calculates the value of H', which is the instantaneous slope of the uniaxial stress versus plastic strain curve. This may be found from equation (A.3) and is given by

$$H' = \frac{d\,Y(\kappa)}{d\,\epsilon_{p,u}} = \frac{1}{A.B}\left(\frac{\epsilon_{p,u}}{A}\right)^{\frac{1-B}{B}} \qquad \text{(A.5)}$$

Subroutine MINV

Two matrix inversion routines which are particularly suitable for the present problem have been programmed and tested. The more accurate of the two empoys full pivotting, but requires more storage and computation time that the other which uses partial pivotting. Both routines will be tested in the overall programme and the better one selected at that time when the accuracy - 'cost' balance can be assessed.

Subroutine TRANS

Here the matrix $[L]^j$ is calculated based on a given set of nodal co-ordinates. This matrix performs the transformation from global to local co-ordinates e.g.

$$\underset{\sim}{q_L} = [L]^j \underset{\sim}{q_G} \qquad \text{(A.6)}$$

Vector algebra is used to form the elements of $[L]^j$.

Subroutine KTRAN

Using the matrix $[L]^j$ computed in subroutine TRANS, this routine sets up the matrix $[T]^e$ given by

$$[T]^e = \begin{bmatrix} L & & & \text{SYMM.} \\ 0 & L & & \\ 0 & 0 & L & \\ 0 & 0 & 0 & L \end{bmatrix} \qquad \text{(A.7)}$$

for a four noded element.

KTRAN then performs the transformation of the elemental stiffness matrix $[K]^e$ from its original axes to global axes, as

$$[K]^e_G = [T]^{e,T} [K]^e_0 [T]^e \tag{A.8}$$

Subroutine ELPL

This subroutine computes the elemental, plastic, pseudo-force vector, $\underset{\sim}{R}^e_L$, from the corresponding incremental, nodal displacement vector $\underset{\sim}{\Delta q}^e_{PL}$. A refined flow chart for ELPL is presented in this report.

The central operation in this subroutine is the integration of the residual (initial) stresses, $\underset{\sim}{\Delta\sigma}^0$, at the stations to yield $\underset{\sim}{R}^e_L$. For each station the amount of computation and storage is great and hence the most suitable quadrature scheme will be the one which uses the minimum number of stations for a given accuracy. The obvious choice, therefore, is Gaussian quadrature, and when we apply it to the present problem we obtain:

$$\underset{\sim}{R}^e_L = \Lambda \sum_{g=1}^{NGPTS} A^g_d \left([N]\,[Q]^g [C]^e\right)^T \underset{\sim}{\Delta\sigma}^g \tag{A.9}$$

where A^g_d is the product of Gauss weights over the area and throughout the thickness at station, g, and Λ is a factor adjusting the limits of integration as those appropriate to the particular element concerned.

Originally it was expected the triangular elements would be the most suitable for use in the analysis, and that seven stations over the area, and a Gauss-Hammer quadrature scheme (71), would be required. However, it now appears that by using quadrilateral elements and just four stations over the area comparable results can be achieved with much

less storage and computation time. This is primarily because the stiffness matrix, $[K]^e$, for a four-noded element is appreciably more accurate than that for a triangle, and it therefore follows that the same is true for the residual stress vector, $\underset{\sim}{\Delta\sigma}^g$, at the chosen number of Gauss stations.

Stress variations through the thickness of the elasto-plastic element are generally more complex than those over the area, and hence in the first tests seven stations through the thickness are being employed. As the first yielding of a panel subjected to lateral loading occurs on the surface, it is desirable that the extreme stations through the thickness are near to the surface in order that the initial yielding is quickly detected. By using seven-point Gaussian quadrature the distance of the outer-most stations from the surface is just 2.5% of the plate thickness.

Subroutine KMAT

This subroutine calculates the elastic stiffness of a triangular or quadrilateral shell element with respect to a global co-ordinate system. The method used is known as the "Hybrid" technique, and the element has been well tested in plate and shell situations.

Subroutine MMAT

This calculates the mass matrix for a general triangular element and transforms it to global axes. The theory is given in Section 7.

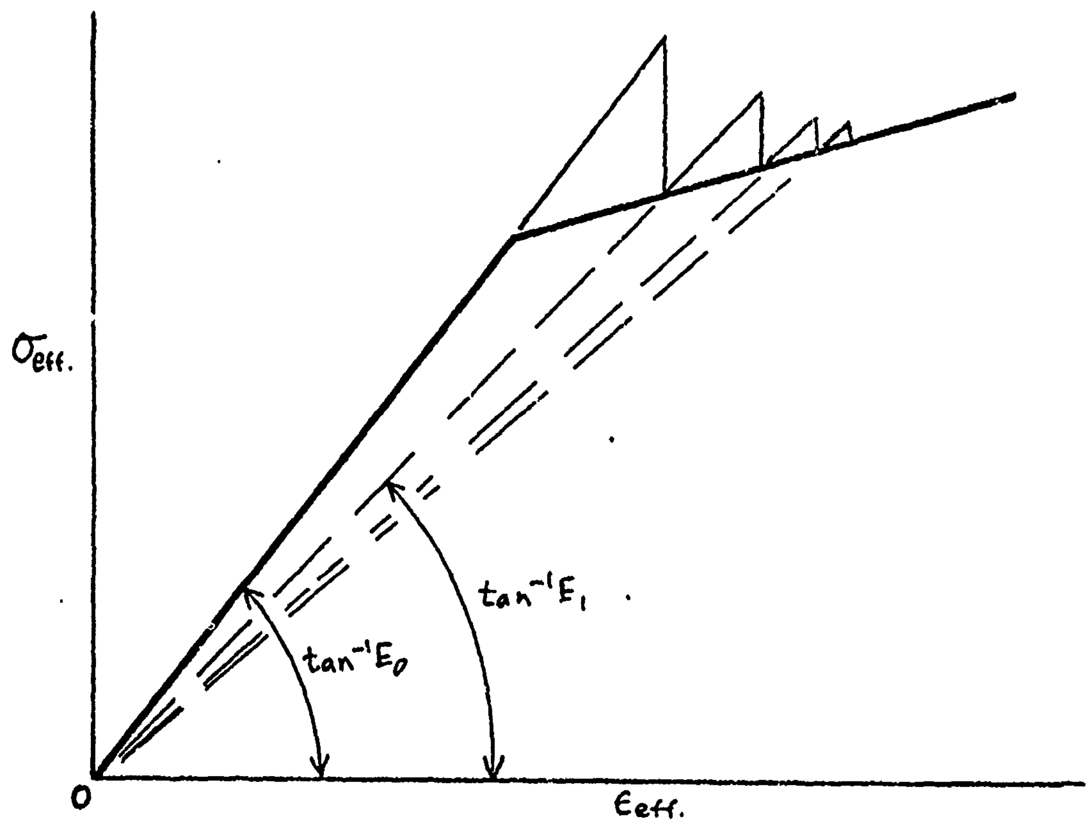

(a) Direct Iterative Approach

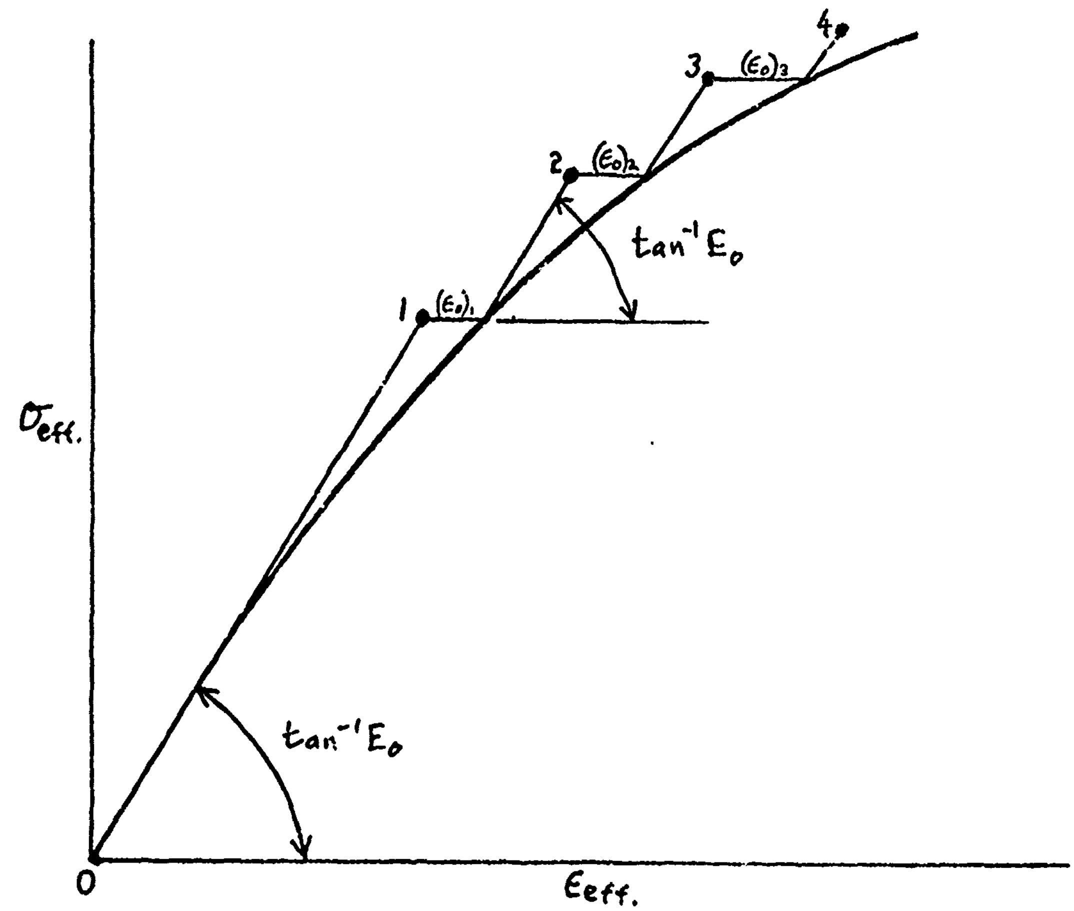

(b) Incremental Initial Strain Approach

Fig. 1 Diagrammatic Representation of Various Finite Element Elasto-Plastic Approaches

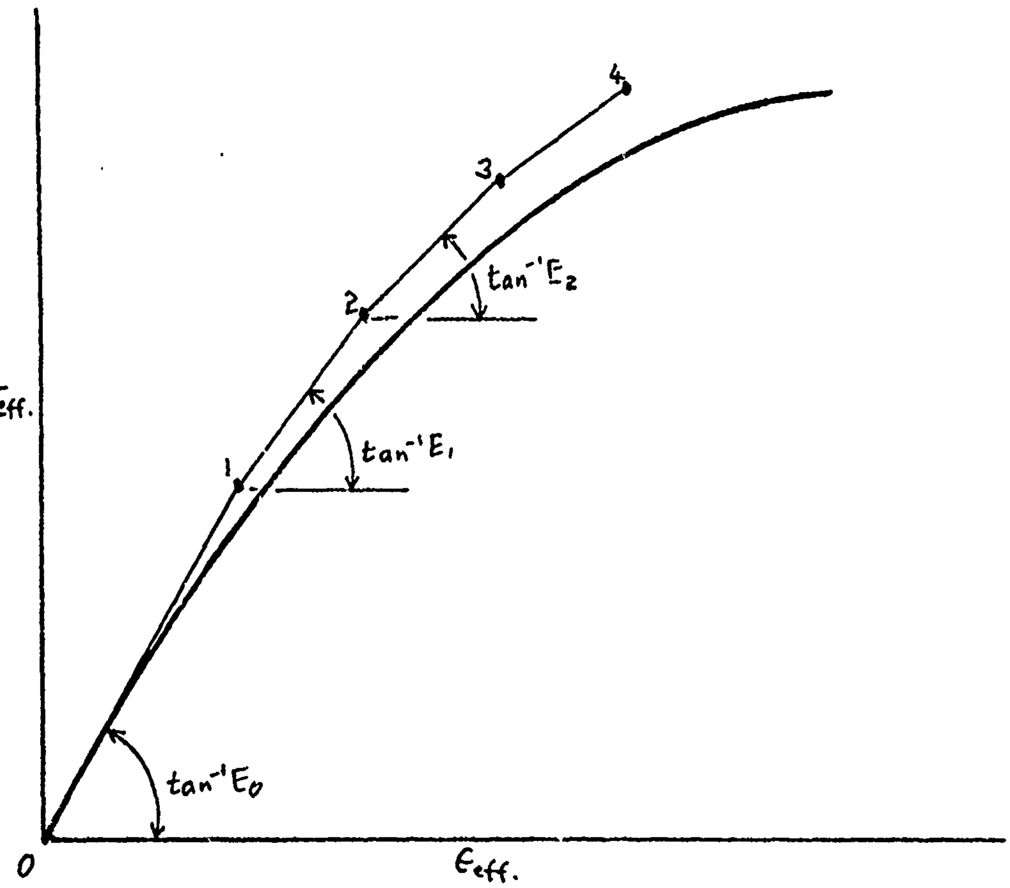

(c) Incremental Tangent Modulus Approach

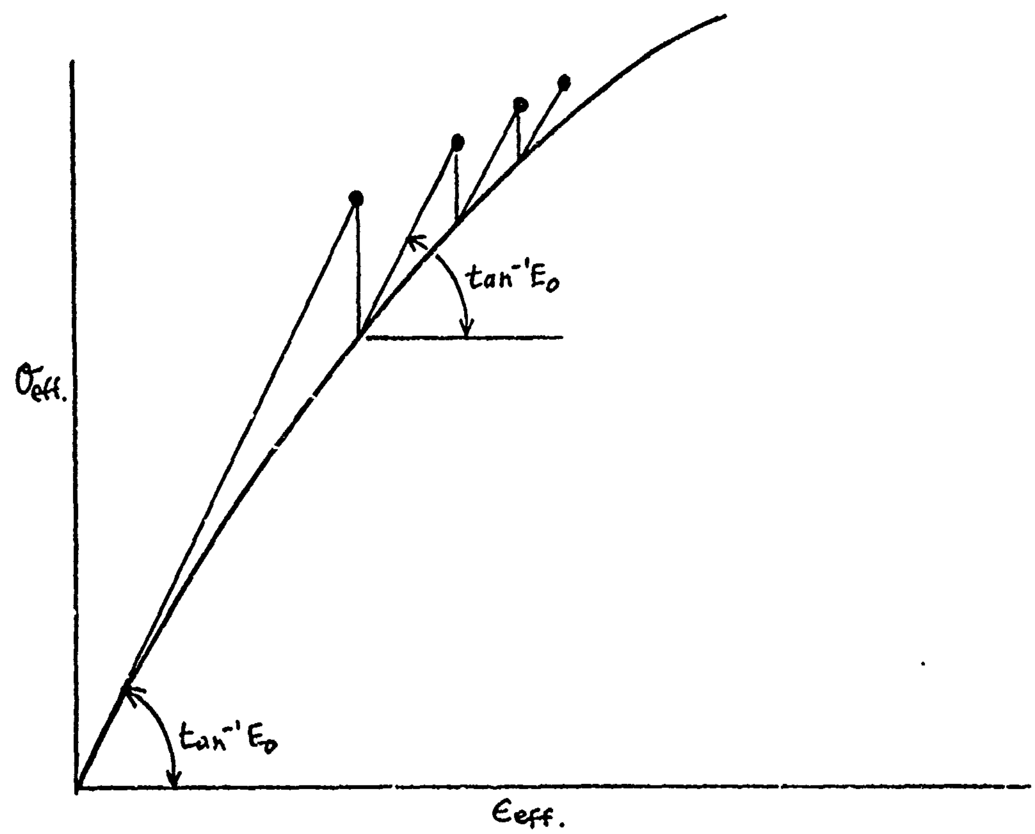

(d) Incremental Initial Stress Approach

Fig. 1 (Continued)

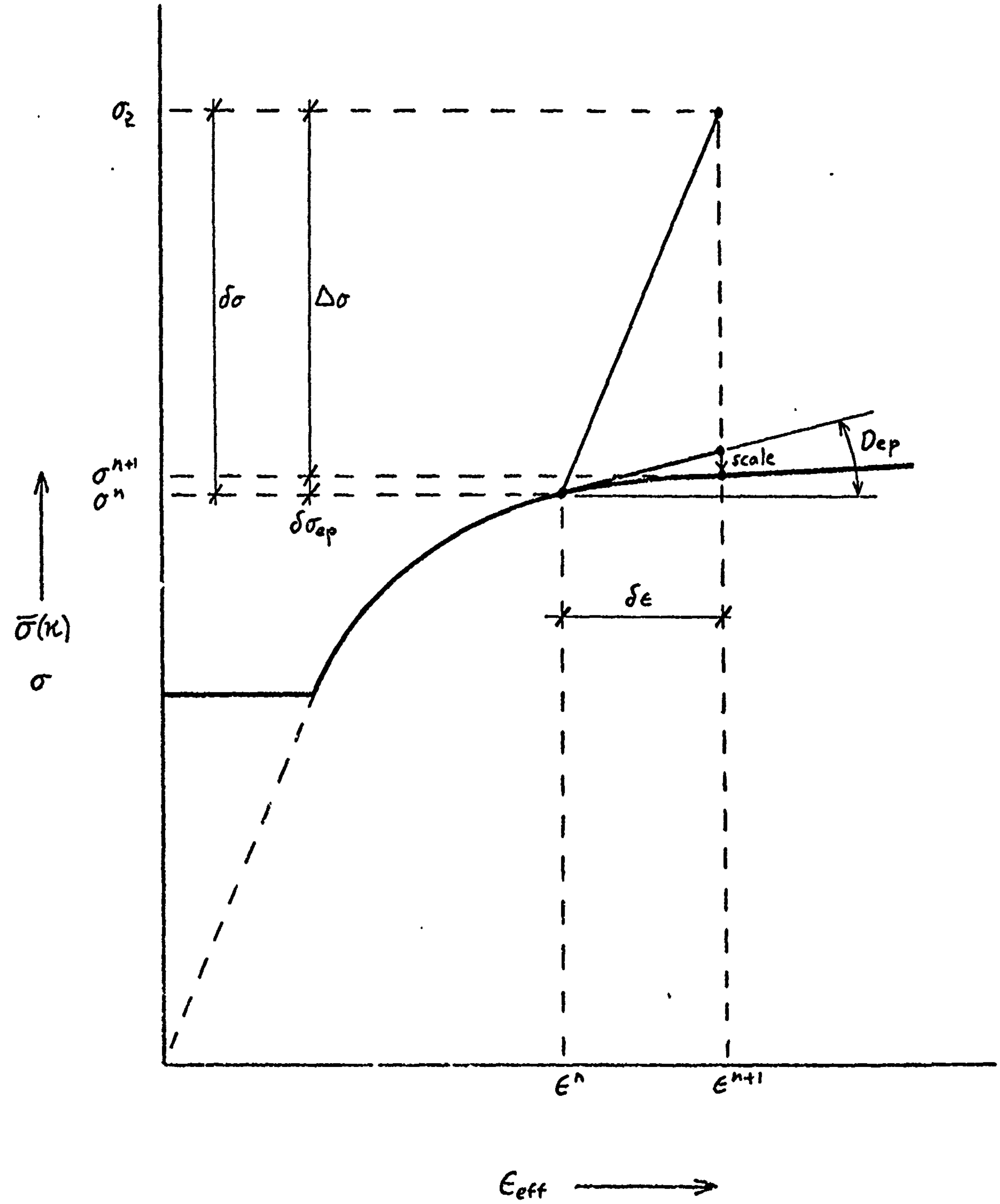

Fig. 2 Diagrammatic Representation of 'Initial Stress' Elasto-Plastic Process for Increment n, n+1

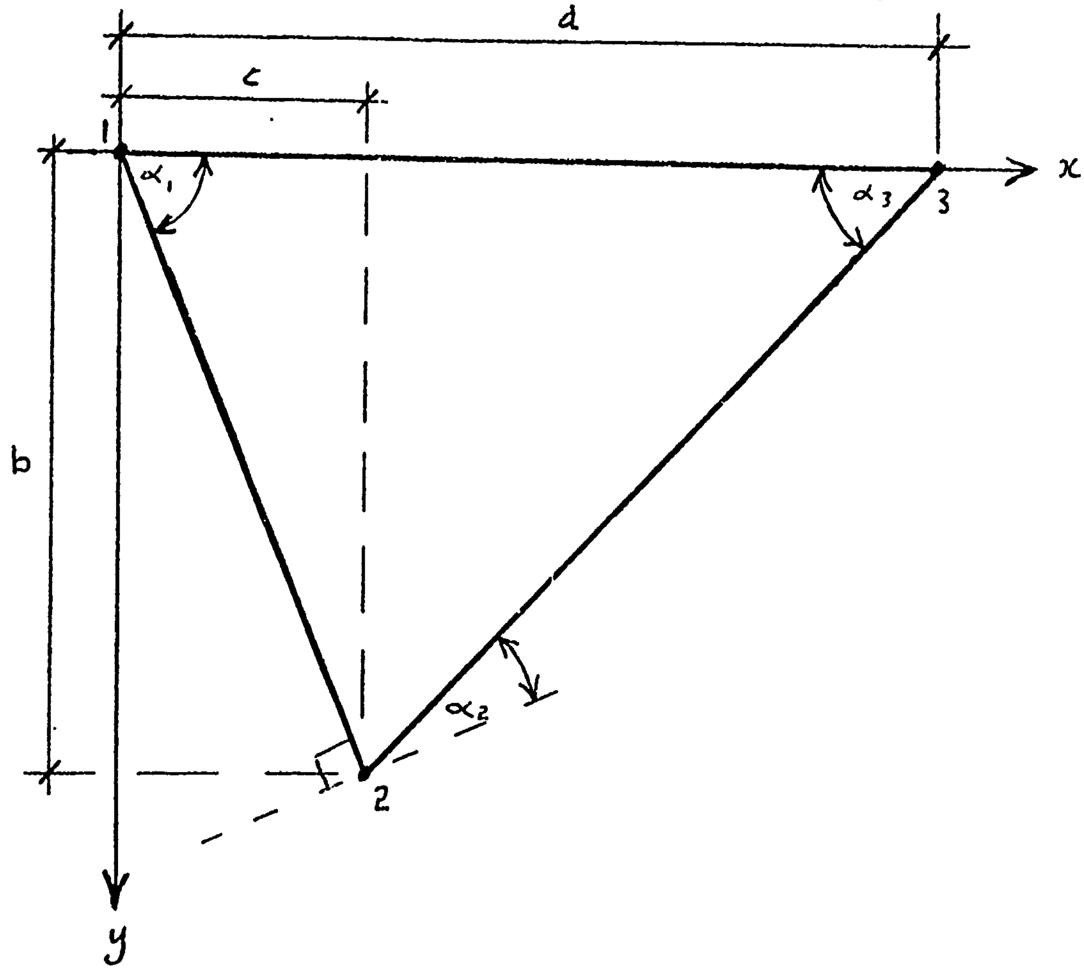

$$l = \frac{c}{a} \qquad i = 1 - l$$

$$ss = \frac{\sin\alpha_1 \, , \, \sin\alpha_2}{\sin\alpha_3}$$

$$sc = \frac{\sin\alpha_1 \, , \, \cos\alpha_2}{\sin\alpha_3}$$

$$cc = \frac{\cos\alpha_1 \, , \, \cos\alpha_2}{\sin\alpha_3}$$

$$cs = \frac{\cos\alpha_1 \, , \, \sin\alpha_2}{\sin\alpha_3}$$

Fig. 3 The General Triangular Element.

$$
\begin{array}{c}
\begin{array}{ccccccccc}
w_1 & \theta_{x_1} & \theta_{y_1} & w_2 & \theta_{x_2} & \theta_{y_2} & w_3 & \theta_{x_3} & \theta_{y_3}
\end{array}\\
\begin{bmatrix}
1 & 0 & 0 & 0 & 0 & 0 & 0 & 0 & 0 \\
0 & 0 & a & 0 & 0 & 0 & 0 & 0 & 0 \\
0 & -b & -ai & 0 & 0 & 0 & 0 & 0 & 0 \\
-3 & 0 & -2a & 0 & 0 & 0 & 3 & 0 & -a \\
0 & b(cc+ss+1) & -ai+b(sc-cs) & 0 & 0 & 0 & 0 & 0 & 0 \\
6i & b & 4ai & 0 & 0 & 0 & -6i & -b & 2ai \\
2 & 0 & a & 0 & 0 & 0 & -2 & 0 & a \\
0 & b(1-cc-ss) & b(cs-sc)+ai & 0 & 0 & 0 & 0 & 0 & 0 \\
6ss-12i & b(4-cc-4ss) & b(4cs-sc)-2ai & 9-6ss & b(cc-2ss)+3b & b(sc-2cs)-3al & 12i-9 & 2b & 3a-4ai \\
-6i & 0 & -3ai & 0 & 0 & 0 & 6i & 0 & -3ai \\
6i-6ss & b(4ss-3+cc) & b(sc-4cs) & 6(ss-1) & b(2ss-cc-2) & -b(sc+2cs)+2al & 6l & -b & -2al \\
12i-6ss & 3b(ss-1) & 3ai-3bcs & 6(ss-1) & 3b(ss-1) & 3al-3bcs & 6-12i & 0 & 3a(2i-1) \\
6(ss-i) & b(2-3ss) & 3bcs-ai & 4-6ss & b(2-3ss) & 3bcs-2al & 6i-4 & 0 & 2a-3ai
\end{bmatrix}
\end{array}
$$

Fig. 4. [V] for General Triangular Element.

$$
a\,b \begin{bmatrix}
A & & & & & & & & & & & & \\
B & C & & & & & & & & & & & \\
E & G & J & & & & & & \text{SYMM.} & & & & \\
C & D & I & E & & & & & & & & & \\
H & J & M & L & \emptyset & & & & & & & & \\
G & I & L & J & \emptyset & N & & & & & & & \\
D & E & J & F & N & K & G & & & & & & \\
J & M & \emptyset & \emptyset & Q & R & Q & S & & & & & \\
J & L & \emptyset & N & R & Q & P & T & T & & & & \\
I & J & N & K & Q & P & M & T & S & Q & & & \\
M & \emptyset & R & Q & T & T & S & V & W & V & Y & & \\
L & N & Q & P & T & S & Q & W & V & U & Y & X & \\
\emptyset & Q & T & S & W & V & U & Y & Y & X & \Omega & Z & \textcircled{H}
\end{bmatrix}
$$

$A = \frac{1}{2}$	$\emptyset = \frac{1}{20}$
$B = \frac{1}{3}$	$P = \frac{1}{21}$
$C = \frac{1}{4}$	$Q = \frac{1}{24}$
$D = \frac{1}{5}$	$R = \frac{1}{25}$
$E = \frac{1}{6}$	$S = \frac{1}{28}$
$F = \frac{1}{7}$	$T = \frac{1}{30}$
$G = \frac{1}{8}$	$U = \frac{1}{32}$
$H = \frac{1}{9}$	$V = \frac{1}{35}$
$I = \frac{1}{10}$	$W = \frac{1}{36}$
$J = \frac{1}{12}$	$X = \frac{1}{40}$
$K = \frac{1}{14}$	$Y = \frac{1}{42}$
$L = \frac{1}{15}$	$Z = \frac{1}{48}$
$M = \frac{1}{16}$	$\Omega = \frac{1}{49}$
$N = \frac{1}{18}$	$\textcircled{H} = \frac{1}{56}$

Fig. 5 $[J_2]$ for General Triangular Element.

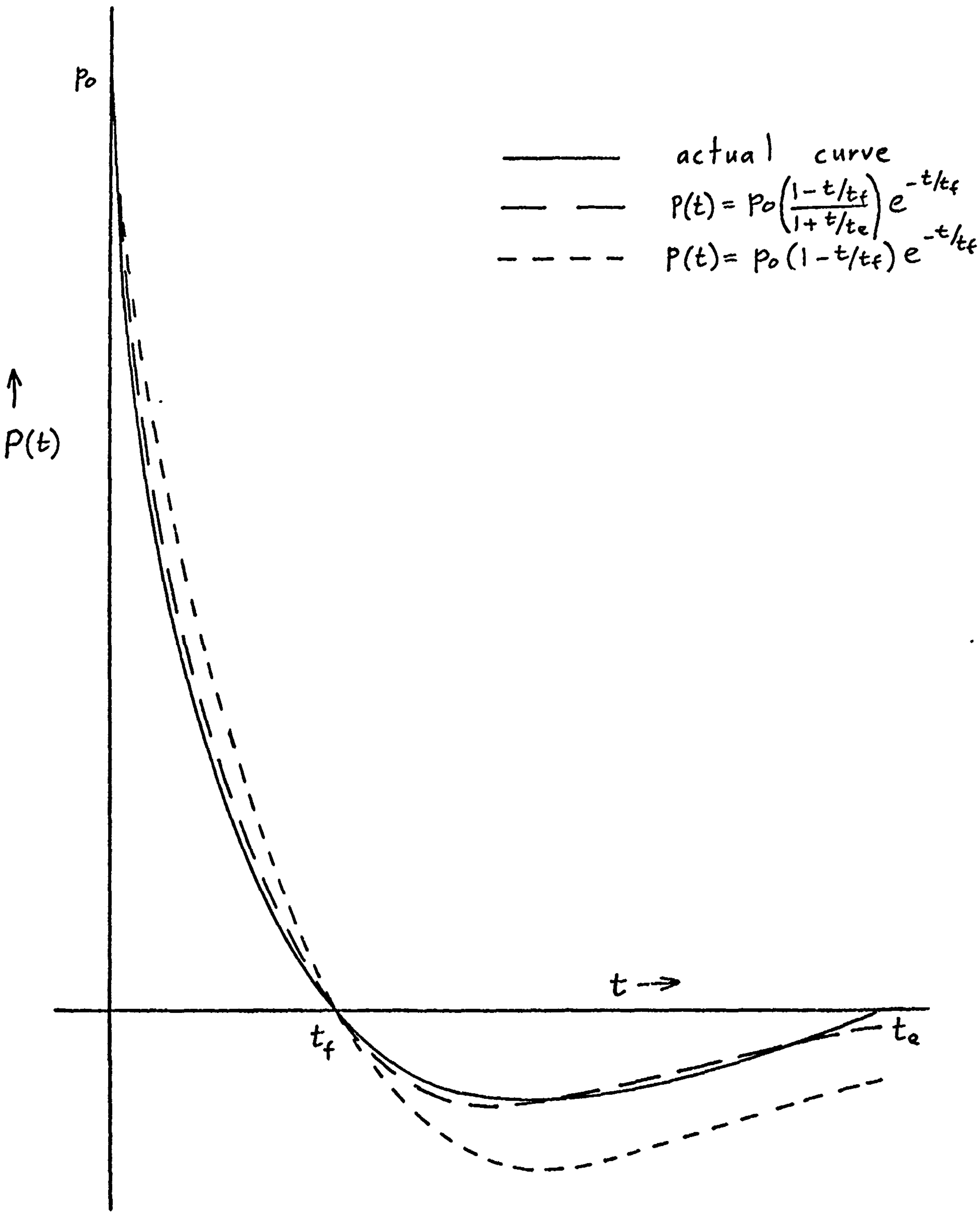

Fig. 6 Representations of Pressure-Time Curve for Blast Loading